UNIVERSITÀ DEGLI STUDI DI PADOVA

DIPARTIMENTO DI BIOLOGIA

Corso di Laurea in BIOTECNOLOGIE

ELABORATO DI LAUREA

Studio dose-effetto di micro-distrofina somministrata per via sistemica nel modello murino mdx della distrofia muscolare di Duchenne

Tutor: Prof. Paolo Laveder
Dipartimento di Biologia

Laureanda: Laura Maurizi Enrici

ANNO ACCADEMICO 2021/2022

ABSTRACT

La distrofia muscolare di Duchenne (DMD) è una rara malattia neuromuscolare degenerativa con meccanismo recessivo legato all'X; mutazioni a livello del gene codificante la distrofina causano la formazione di una proteina tronca non funzionale o l'assenza della proteina stessa.

Per il ripristino della proteina carente è stato progettato rAAVrh74, un vettore di virus adeno-associato (AAV), di cui si segnala l'assenza di tossicità, contenente un transgene della micro-distrofina umana la cui sequenza è stata indirizzata per mezzo di un promotore specifico per il muscolo scheletrico e cardiaco, MHCK7.

Per testare l'efficacia di rAAVrh74.MHCK7.micro-distrofina, sono state valutate iniezioni sistemiche nei topi mdx a dosi basse, intermedie ed elevate.

A tre mesi dall'inizio del trattamento, la forza specifica è aumentata nel diaframma e nel muscolo tibiale anteriore, con dosi intermedie, raggiungendo i livelli osservati nel topo wild type. A livello istologico si osserva, in particolar modo nel diaframma, una riduzione della fibrosi e la normalizzazione delle dimensioni delle miofibre.

In definitiva, questo studio preclinico dimostra la sicurezza e l'efficacia della somministrazione sistemica del vettore rAAV.MHCK7.micro-distrofina ad alte dosi, a sostegno dell'inizio di uno studio di Fase I/II sull'applicazione del metodo in sicurezza nei pazienti umani con DMD.

SOMMARIO

Sommario

1. STATO DELL'ARTE

DISTROFIA MUSCOLARE DI DUCHENNE

La distrofia muscolare di Duchenne (DMD) è la più nota e diffusa malattia neuromuscolare a esordio infantile. Questa malattia genetica recessiva legata all'X provoca atrofia muscolare progressiva, insufficienza cardiaca e respiratoria.
Nei primi stadi della malattia, intorno ai 3-5 anni di età, i pazienti presentano i primi sintomi quali debolezza agli arti inferiori, andature anormali e pseudo-ipertrofia del muscolo del polpaccio, le quali causano continue cadute. Entro i 12 anni si diventa completamente dipendenti dalla sedia a rotelle andando quindi incontro a ventilazione assistita entro i 20 anni e infine a morte entro i 30-40 anni. Questa patologia viene riscontrata in individui che presentano mutazione a livello del gene DMD, il quale codifica per la proteina distrofina (Dp427m); è stato infatti osservato che oltre 4.000 mutazioni a livello di questo gene causano l'assenza di espressione di distrofina funzionale. Poiché il gene della distrofina è sul cromosoma X, le mutazioni nel gene della distrofina portano a una produzione di distrofina non funzionale in circa 1 maschio su 5.000

- **Struttura della distrofina**

Il gene DMD è localizzato nel braccio corto del cromosoma X in posizione p21.2 e rappresenta uno dei geni più grandi del genoma umano, circa 2,2 Mb (cioè circa lo 0,1% dell'intero genoma umano). La parte codificante del gene è composta da 79 esoni, che formano una proteina di 427 kDa (Dp427m); tuttavia, il 99% della sequenza genica è rappresentata da introni di grandi dimensioni.
La distrofina è localizzata sotto la membrana cellulare delle fibre muscolari striate, il sarcolemma, dove, attraverso quattro domini essenziali (Figura 1.1), interagisce con il sarcolemma stesso e il citoscheletro (microfilamenti di actina, filamenti intermedi, microtubuli e altre proteine strutturali correlate).
La distrofina e le proteine a cui si lega formano il complesso di membrana distrofina-glicoproteina (DGC). Il DGC contiene undici proteine: distrofina, il sottocomplesso del distroglicano (α-distroglicano e β-distroglicano), il sottocomplesso del sarcoglicano (α-sarcoglicano, β-sarcoglicano, γ-sarcoglicano e δ-sarcoglicano), sarcospan, sintrofina, distrobrevina e nitrico neuronale ossido sintasi (nNOS).

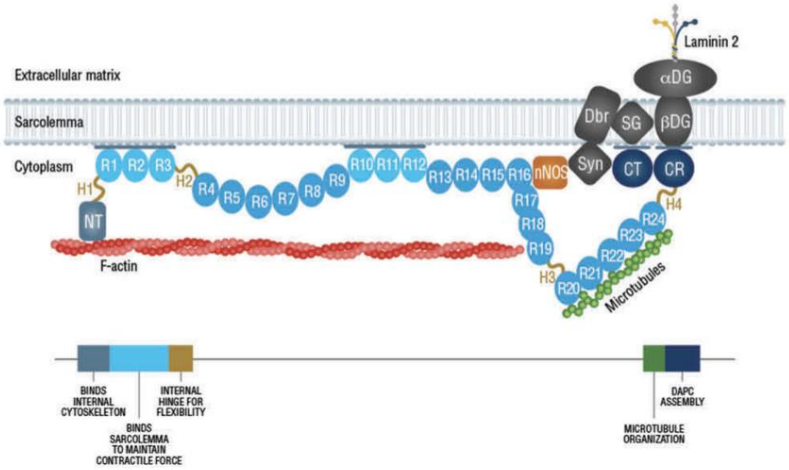

***Figura 1.1**; Il primo domino, dominio amminico terminale legante l'actina N-term, collega la distrofina ai filamenti di actina sottosarcolemmale; il dominio centrale dell'asta della distrofina contiene 24 ripetizioni di circa 109 amminoacidi, con cui si lega al sarcolemma, all'actina, ai microtubuli, al β-destroglicano e ad altre proteine. Il dominio del bastoncello interagisce con i microtubuli e i fosfolipidi di membrana; per mezzo di questo dominio la distrofina ha una maggiore elasticità. Il terzo dominio è il dominio ricco di cisteina situato tra il dominio bastoncello e il dominio terminale carbossilico. Il quarto e ultimo dominio della distrofina è il dominio terminale carbossilico C-term il quale fornisce anche siti di legame per la sintrofina e la distrobrevina.*

Due regioni del gene DMD sono considerate hotspot per le mutazioni.
La prima è tra gli esoni 45 e 55; infatti, delezioni in questa zona provocano la rimozione della parte centrale del dominio dell'asta.
Il secondo hotspot si ha tra l'esone 3 e l'esone 19. Delezioni in questa zona causano la rimozione parziale o totale del dominio amminico terminale legante l'actina e una porzione del dominio del bastoncello.
Alcune delezioni di esoni inducono una mutazione frameshift, alterando quindi la funzione della distrofina. Circa il 60-70% delle mutazioni nei pazienti con DMD sono delezioni esoniche, il 5-15% sono duplicazioni e il 20% sono mutazioni puntiformi, piccole delezioni o inserzioni.

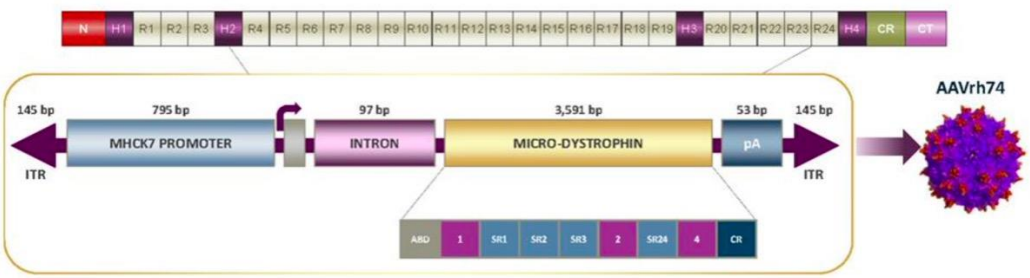

***Figura 1.2**. Struttura della micro-distrofina clonata nel vettore AAVrh74*

- **Patogenesi della malattia**

Nel muscolo normale, il sarcolemma è in grado di resistere a stress meccanici dati dalla contrazione e dal rilassamento delle fibre grazie alle numerose interazioni tra i filamenti contrattili e il complesso DGC. L'assenza di distrofina, viceversa, causa instabilità del DGC: il sarcolemma non interagisce bene con il citoscheletro, diventando quindi più suscettibile ai danni provocati dalla contrazione. Il danno muscolare, correlato allo stress muscolare, colpisce i muscoli più sollecitati, come il diaframma (DIA), il quale è il muscolo principale di ventilazione a riposo.

Le fibre muscolari danneggiate sono rilevate da cellule del sistema immunitario (macrofagi e cellule T, neutrofili, mastociti ed eosinofili), le quali contribuiscono all'infiammazione. A differenza del muscolo normale che presenta miofibre ben organizzate e uniformi con nuclei posizionati perifericamente, il muscolo distrofico è caratterizzato invece da una disorganizzazione delle miofibre, nuclei localizzati centralmente e un'abbondante infiltrazione di cellule infiammatorie.

La capacità rigenerativa del muscolo sano è data dalla presenza di cellule satelliti funzionali; queste cellule staminali adulte del tessuto scheletrico, presenti tra la lamina basale e il sarcolemma della fibra muscolare, nel muscolo sano compiono la rigenerazione in risposta a lesioni muscolari. Esse rimangono quiescenti finché non vengono attivate da fattori come esercizio o traumi.

Nelle fibre muscolari danneggiate, in condizioni normali le cellule satelliti si dividono in modo asimmetrico per generare sia una cellula in attiva divisione sia per mantenere integro il pool di cellule satellite. In assenza di distrofina questo meccanismo è alterato, causando quindi la loro deplezione.
Quando il pool di cellule satellite è esaurito, il muscolo danneggiato è sostituito con tessuto fibrotico e adiposo portando al progressivo deterioramento della qualità muscolare e alla perdita di massa muscolare. Inoltre, nel muscolo malato si ha una deposizione eccessiva di proteine della matrice extracellulare (ECM) da parte dei fibroblasti, alterando così la funzionalità muscolare.

Infine, nel sangue di pazienti distrofici si rilevano alti livelli di creatina chinasi (CKM, isoforma muscolare). Questo enzima è fondamentale per l'accumulo e il rilascio di energia a livello dei muscoli; i danni muscolari compromettono l'integrità del sarcolemma e causano il rilascio di CKM nel sangue.

2. APPROCCIO SPERIMENTALE

- **Modello animale**

Tra i topi mdx, il modello C57BL/10ScSn è il più utilizzato per lo studio dell'DMD.
I livelli di creatinchinasi molto elevati osservati inizialmente nel sangue, fecero presupporre che ci fosse un danno muscolare; infatti, si osservò la presenza di una mutazione puntiforme (transizione da C a T) nell'esone 23 del gene DMD, la quale ha portato all'assenza della distrofina a lunghezza intera, causando così i tipici segni distintivi della distrofia muscolare. Come controllo è stato utilizzato il topo C57BL/6 wild type.
Tutti i topi utilizzati nello studio preclinico erano maschi di età compresa tra le 4 e le 5 settimane. Tutte le procedure sono state approvate dall'Istituto di ricerca presso il Comitato istituzionale per la cura e l'uso degli animali del *Nationwide Children's Hospital*. I due ceppi di topo, allevati e mantenuti come animali omozigoti in condizioni standardizzate nell'*Animal Resources Core* presso l'Istituto di ricerca del *Nationwide Children's Hospital,* sono stati mantenuti su *Teklad Global Rodent Diet* (3,8% di fibre, 18,8% di proteine, 5% di cibo grasso) con un ciclo di 12 ore di buio/12 ore di luce.

- **Produzione di rAAV**

I virus adeno-associati (AAV) sono attualmente i vettori preferiti per terapia genica, in quanto hanno bassa patogenicità e, rispetto ad altri vettori virali utilizzati per la terapia genica (ad esempio, adenovirus) alcuni sierotipi hanno un trofismo muscolare naturale. Inoltre, sono in grado di infettare cellule sia in attiva divisione che quiescenti. I virus adeno- associati sono dei piccoli virus (circa 20 nm) a DNA a singolo filamento non dotati di *envelope*. A causa della loro incapacità di imballaggio, sono state prodotte delle forme troncate della proteina distrofina le quali hanno conservato domini di legame distali cruciali.
I transgeni codificanti la micro-distrofina (sono circa un terzo rispetto al gene della distrofina a lunghezza intera, vedi Figura 1.2) sono stati sviluppati e studiati in modelli murini e cani che presentavano distrofia muscolare di Duchenne.
Il vettore wild type presenta un gene Rep per la replicazione virale e un gene Cap per generare il capside virale; contiene inoltre due ripetizioni terminali invertite (ITR), posizionate alle estremità del genoma virale.
L'ITR funge da origine di replicazione e segnale di confezionamento. Nel rAAV (virus adeno-associato ricombinante) la cassetta di espressione terapeutica sostituisce i geni Rep e Cap wild-type. L'unico componente virale nel genoma rAAV è l'ITR (145 nucleotidi ciascuno).
Il metodo di produzione del vettore AAV più comunemente usato è il sistema di tripla trasfezione transitoria. Un plasmide AAV cis-acting porta la cassetta di

espressione AAV contenente il gene di interesse fiancheggiato dagli ITR. Un plasmide trans Rep/Cap esprime la replicazione e le proteine del capside. Poiché il ciclo di vita riproduttivo di AAV richiede l'aiuto dell'adenovirus, un plasmide helper dell'adenovirus è incluso nel cocktail di trasfezione.

- **Sierotipo rh74**

L'AAVrh74 (sierotipo AAV rh74) utilizzato negli esperimenti è stato isolato dai linfonodi delle scimmie rhesus, poiché si era osservato l'alto tropismo per il muscolo scheletrico e cardiaco. Essendo di origine non umana, AAVrh74 riduce la probabilità che i pazienti abbiano un'immunità preesistente al vettore. Ad oggi, AAVrh74 è risultato sicuro e tollerabile negli studi sull'uomo, con una risposta immunitaria minima.

- **Costruzione del transgene**

Come precedentemente accennato, il dominio C-terminale della distrofina si lega a due componenti del complesso DGC, la sintrofina e la distrobrevina.
Dopo aver generato ceppi di topo mdx transgenici che esprimono le distrofine delete del dominio di legame per sintrofina o il dominio di legame della distrobrevina, si osserva una normale funzione muscolare e una localizzazione essenzialmente normale di sintrofina e distrobrevina. Perciò si è notato che la sintrofina e la distrobrevina possono legarsi al complesso DGC indipendentemente dalla distrofina e che questa associazione è sufficiente per prevenire la distrofia.
Una porzione del dominio C-terminale (822 bp), corrispondente agli esoni 71–78, è stata quindi eliminata dal cDNA della distrofina murina a lunghezza intera mediante PCR ricombinante, lasciando gli ultimi tre amminoacidi (esone 79) della proteina distrofina inalterati. Inoltre, sono state rimosse delle porzioni (878 bp) delle regioni 5' e 3' non tradotte (UTRs). È stato progettato il Kozak consensus per aumentare l'efficienza della traduzione ed è stato introdotto un introne SV40, per aumentare l'espressione del transgene, e una sequenza poliA.
La cassetta MHCK7 consente un'espressione elevata e allo stesso tempo specifica per il muscolo scheletrico e cardiaco: si combina infatti la potente cassetta muscolare CK7 con il potenziatore del gene α-MHC cardiaco. Il potenziatore del complesso della catena pesante α-miosina del topo (α-MHC) da 188 bp, noto per conferire un'attività specifica nel muscolo cardiaco, è stato legato alla cassetta CK7 con orientamenti positivi e negativi per creare le cassette MHCK7 da 770 bp.
Oltre ad aumentare l'attività della cassetta di circa 2 volte nei miociti scheletrici, questa modifica ha portato anche a un aumento di circa 5 volte dell'attività nei cardiomiociti.
In uno studio precedente sono state create tre differenti micro-distrofine; la proteina mancante della porzione ΔR4-R23 era la più efficiente e i muscoli di questi

topi erano morfologicamente normali, perciò, si è deciso di eliminare anche questa porzione.

- **Delivery *in vivo* nei topi mdx**

Dopo esser stati randomizzati in ordine sequenziale e dosati per peso corporeo medio per gruppo, i topi mdx sono stati trattati o con Ringer lattato (mdx-LR, n=6) o con rAAVrh74.MHCK7.micro-distrofina a dosi crescenti: 2×10^{12} dose totale vg, 8×10^{13} vg/kg (n= 5); 6×10^{12} vg dose totale, 2×10^{14} vg/kg (n= 8); o $1{,}2 \times 10^{13}$ vg dose totale, 6×10^{14} vg/kg (n = 8) per via endovenosa attraverso la vena della coda.
Un'altra coorte di topi è stata trattata con la dose intermedia (6×10^{12} vg)(n =8).
I primi topi sono stati sottoposti a necroscopia a 12 settimane dopo la somministrazione del vettore, mentre i topi trattati separatamente sono stati sottoposti a necroscopia a 24 settimane dalla somministrazione del vettore per svolgere un'analisi istologica, funzionale e di espressione a lungo termine.
I dati sono stati raccolti ed elaborati senza sapere a che coorte si riferissero.

- **Ematologia**

Dopo aver prelevato il sangue tramite una puntura cardiaca, è stata svolta l'analisi del siero. Il sangue dei topi mdx, wild type, trattati con LR, dose intermedia (6×10^{12} vg) e dose elevata ($1{,}2 \times 10^{13}$vg) è stato raccolto in una provetta di separazione del siero e centrifugato per 10 minuti a 15.000 rpm. Il surnatante raccolto è stato congelato e inviato ai *Charles River Laboratories* per i test clinici, dando priorità agli enzimi epatici a causa dello scarso volume ottenuto.

- **Immunofluorescenza**

Le criosezioni (12 µm) dei muscoli tibiale anteriore (TA), gastrocnemio (GAS), quadricipite (QD), psoas major (PSO), gluteo (GLUT), tricipite (TRI) e diaframma (DIA) insieme al cuore, sono state sottoposte a colorazione immunofluorescente per la micro-distrofina. È stato utilizzato un anticorpo primario anti-distrofina umana monoclonale murino (Santa Cruz Biotechnology, Dallas, TX) a una diluizione di 1:50 e l'anticorpo primario umano anti-β-sarcoglicano (Leica Biosystems, Buffalo Grove, IL) a una diluizione di 1:100.

- **Contrazione tetanica del diaframma**

A seguito dell'eutanasia, il diaframma (DIA) è stato rimosso dai topi con attacchi costali e tendine centrale intatti e collocato nel tampone Kreb's-Henseleit (KH) (95% O_2 /5% CO_2 (pH 7,4), 118 mmol/L NaCl , 25 mmol/L $NaHCO_3$, 5 mmol/L KCl, 1 mmol/L KH_2PO_4 , 2 mmol/L $CaCl_2$, 1 mmol/L $MgCl_2$, 5 mmol/L glucosio)

Un'estremità del muscolo è stata legata tramite filo da sutura a un perno rigido mentre l'altra estremità è stata legata a un trasduttore di forza-servomotore a doppia modalità (305C; Aurora Scientific, Aurora, Ontario, Canada), all'interno di un bagno riempito con una soluzione mantenuta a 37°C. Tramite due elettrodi a piastra di platino il muscolo è stato disteso finché non è stata raggiunta una lunghezza in cui le contrazioni erano ottimali.
In seguito alla stabilizzazione del muscolo, il diaframma è stato sottoposto a un protocollo costituito da una serie di 6 contrazioni tetaniche, 3 contrazioni da 1 Hz ogni 30 s, seguite da 3 contrazioni da 150 Hz ogni minuto. Dopo un periodo di riposo di 3 minuti, il DIA è stato stimolato a 20, 50, 80, 120, 150 e 180 Hz, facendo riposare il muscolo per due minuti tra uno stimolo e l'altro, ciascuno con una durata di 250 ms, per determinare la forza tetanica massima.
Le misurazioni della forza sono state normalizzate all'area della sezione trasversale, determinata dopo aver calcolato la lunghezza e il peso del muscolo.

- **Contrazione tetanica tibiale anteriore per la valutazione funzionale**

I topi sono stati anestetizzati usando una miscela di ketamina/xilazina. Il tendine TA distale e il nervo sciatico sono stati esposti per le successive operazioni.
Il topo è stato trasferito su una pedana termocontrollata. Dopo aver legato tramite una sutura ad anello il tendine AT distale al braccio di livello del trasduttore di forza e fissato il nervo sciatico agli elettrodi, il muscolo è stato stabilizzato.
Per determinare la tensione ottimale da utilizzare durante la procedura, la tensione a riposo è stata impostata su 2, 3, 4, 5 e 6 g di forza e stimolata a 1 Hz (la corrente è stata impostata su 200 mA per la durata delle analisi). Dopo un periodo di riposo di 3 minuti, l'AT è stato stimolato a 50, 100, 150 e 200 Hz, facendo riposare il muscolo per un minuto tra uno stimolo e l'altro. Dopo un riposo di 5 minuti, i muscoli sono stati quindi sottoposti a una serie di 10 contrazioni isometriche, a intervalli di 1 minuto con una procedura di allungamento-riallungamento del 10%. Dopo le contrazioni eccentriche, i topi sono stati soppressi e il muscolo TA è stato sezionato e congelato per l'istologia.

- **Analisi Western blot**

Dopo l'estrazione dai campioni muscolari, le proteine (50 g per muscoli e organi) sono state separano mediante elettroforesi su SDS-PAGE (gel con gradiente Novex NuPAGE 3-8%, Invitrogen, Waltham, MA) e sono state trasferite su membrana di fluoruro di polivinilidene. Queste sono state sondate con l'anticorpo primario anti-distrofina Dys1 per il rilevamento della distrofina e Dys3 per la micro-distrofina (Leica Biosystems) a una diluizione di 1:50 e 1:20, rispettivamente, e l'anticorpo primario dell'ossido nitrico sintasi neuronale (nNOS) (Fisher Scientific) a un diluizione di 1:1.000. I controlli di caricamento utilizzati includevano l'anticorpo γ-

tubulina (Sigma) e l'anticorpo α-actinina (Sigma) a una diluizione di 1:10.000 seguiti da Alexa Fluor 680 (1:5.000, LI-COR, Lincoln, Nebraska).

- **Analisi morfometrica**

Le criosezioni muscolari di 12 μm di topi WILD TYPE, animali mdx-LR e topi mdx trattati con rAAVrh74.MHCK7.micro-distrofina sono state colorate con ematossilina ed eosina per l'esame. In tutti i muscoli è stato misurato il diametro delle fibre muscolari utilizzando quattro campi di ingrandimento 20X per animale, per lato e per tessuto. Per muscolo, sono state misurate 1.000-5.000 fibre da ciascun gruppo di trattamento e coorte di controllo. Per i muscoli TA, GAS, QD, PSO, GLUT, TRI e DIA, sono stati analizzati quattro campi di ingrandimento dell'immagine 20X dal lato sinistro dell'animale per valutare la proporzione di miofibre con nuclei centrali.

- **Analisi qPCR della biodistribuzione**

La TaqMan qPCR permette di contare il numero di copie vg presenti sia nel muscolo target, sia negli organi out of target. L'analisi di biodistribuzione è stata eseguita su tre topi mdx per ogni livello di dose. I tessuti si raccolgono durante l'autopsia, dopo estrazione del DNA si utilizzano set di primer specifici per una sequenza unica della regione intronica a valle del promotore MHCK7. Qualsiasi rilevamento di più di cento copie di DNA a filamento singolo per grammo di DNA genomico si considera un segnale positivo. Il numero di copie del DNA genomico è indicato come vg/g.

- **Colorazione rossa di Picrosirius e quantificazione del collagene**

Sezioni di muscolo DIA caricate su vetrini da microscopio *Fisherbrand Superfrost* sono state congelate e fissate in formalina tamponata neutra al 10% per 5 minuti prima di essere risciacquati in acqua distillata. I vetrini sono stati incubati per 15 minuti nella soluzione B (Direct Red 80/2 4 6-trinitrofenolo) del *Picrosirius red stain kit* (Polysciences, Inc.), risciacquati in acqua distillata e poi incubati nella soluzione C (acido HCl 0,1 N). Di seguito è avvenuta la colorazione per 5 minuti con Fast Green all'1% in acido acetico glaciale, usando una diluizione 1:10 di acqua deionizzata. Infine, i vetrini sono stati nuovamente risciacquati in acqua distillata, disidratati in etanolo, chiarificati in xilene e montati con vetrini coprioggetto.

- **Analisi statistica**

I dati sono espressi come media ± errore standard della media (SEM, barre di errore). È stato utilizzato il test ANOVA per l'analisi della varianza unidirezionale e un ANOVA a due vie per confronti multipli tra gruppi indipendenti tra loro.

3. RISULTATI E DISCUSSIONE

- **Miglioramenti istologici con somministrazione sistemica in modo dose-dipendente**

I topi sono stati suddivisi in tre coorti; i topi di ciascuna coorte sono stati trattati con una dosa totale bassa, media o alta di rAAVrh74.MHCK7.micro-distrofina. Il vettore è stato somministrato per via endovenosa nella vena della coda di topi mdx di quattro o cinque settimane di età.

A tre mesi dalla somministrazione sistemica di rAAVrh74.MHCK7.micro-distrofina, i topi sono stati sottoposti a necroscopia e analizzati tramite immunofluorescenza. L'espressione del transgene della micro-distrofina è stata esaminata mediante immunoistochimica nei muscoli scheletrici del lato sinistro e destro, inclusi TA, GAS, QD, PSO, TRI e GLUT, oltre al cuore e il DIA (Figura 3.1, A).

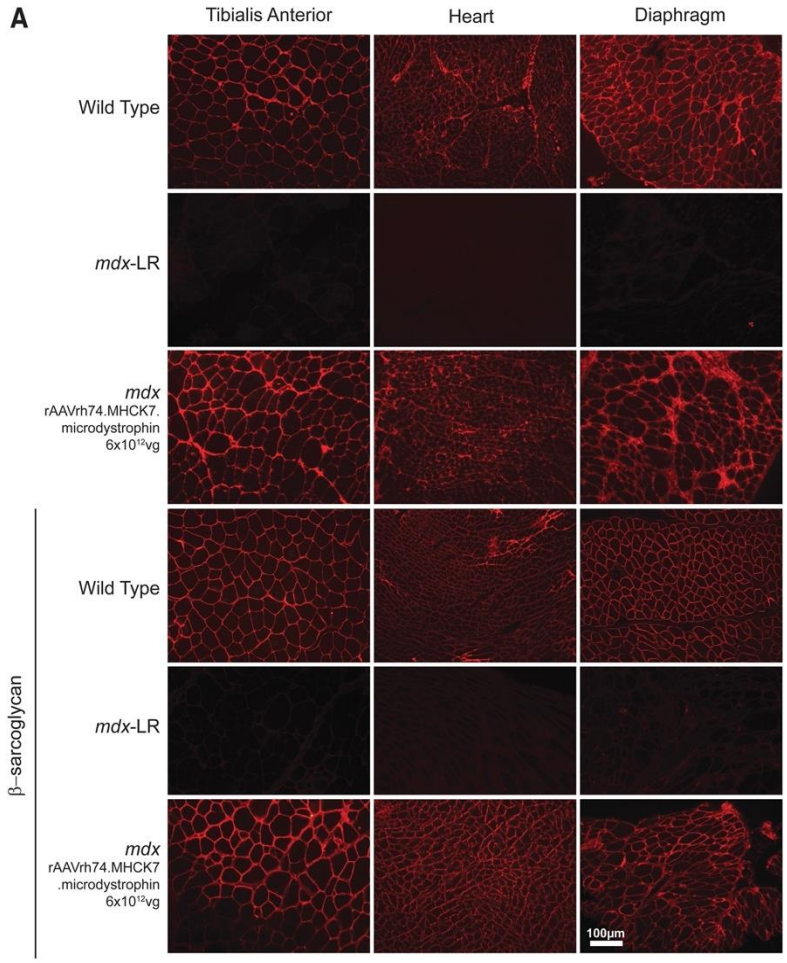

Figura 3.1
(A) Immunoistochimica del muscolo tibiale anteriore, del cuore e del diaframma di topo WILD TYPE, mdx-LR e mdx trattato con il transgene rAAVrh74.MHCK7.micro distrofina alla dose intermedia di 6 × 10^{12} vg. L'espressione del β-sarcoglicano rappresenta il salvataggio del complesso proteico associato alla distrofina.

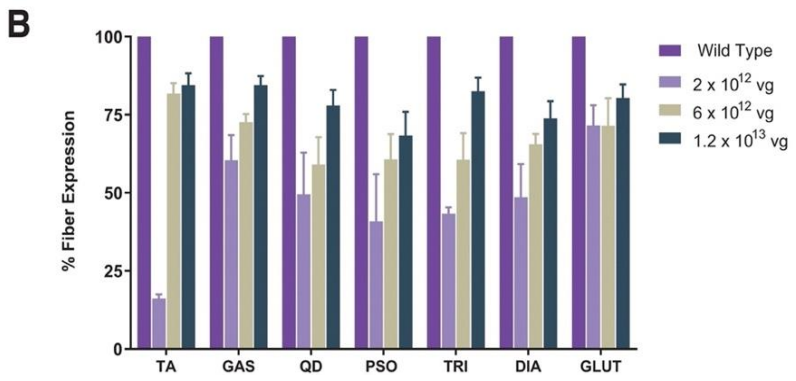

Figura 3.1
(B) Percentuale di fibre di TA, GAS, QD, PSO, TRI, DIA e GLUT che esprimono la micro-distrofina

L'immunoistochimica dimostra una robusta espressione di micro-distrofina sulla membrana del sarcolemma del muscolo scheletrico e cardiaco. Inoltre, dopo il trasferimento del gene della micro-distrofina, l'espressione del β-sarcoglicano è stata ripristinata. Come si può notare, a tre mesi dalla somministrazione il livello di espressione della micro-distrofina ha avuto un notevole miglioramento nel cuore dei topi trattati con dosi intermedie, raggiungendo quasi i livelli di espressione nel topo wild type (Figura 3.1, B).

Poiché nel processo distrofico croniche sono state osservate fibrosi e infiammazioni, sono stati valutati il diametro della fibra, la fibrosi e la nucleazione centrale (CN) in seguito alla somministrazione del vettore in dosi intermedie e alte rispetto ai topi mdx-LR (Figura 3.2, A).

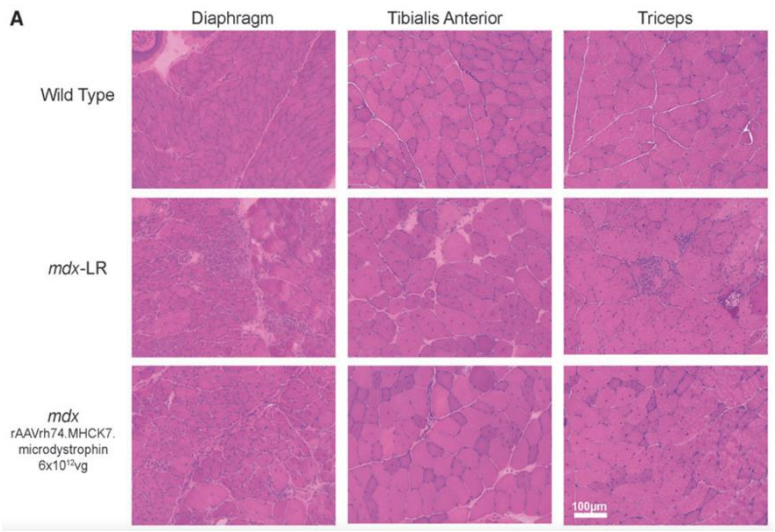

Figura 3.2
(A) Colorazione con ematossilina ed eosina del DIA, del TA e del TRI di topo WILD TYPE, mdx-LR e topo trattato con rAAVrh74.MHCK7.micro-distrofina alla dose intermedia (6 × 10 ^{12} vg).

In topo trattati con dosi di vettore intermedie e alte è stata accertata una riduzione significativa della gravità patologica e delle caratteristiche distrofiche, come la

fibrosi, oltre che l'aumento significativo del diametro delle fibre (Figura 3.2, B-C). Le fibre del DIA di topo trattati con dosi basse e intermedie hanno diametro simile a quello delle fibre del DIA wild type, mentre è stata osservata una normalizzazione della dimensione delle fibre nel TA di topi in cui erano state somministrate dosi basse e alte e nel TRI di topi trattati con la dose intermedia.
La quantificazione dei parametri istologici ha dimostrato una significativa riduzione del CN in tutti i muscoli scheletrici analizzati in modo dose-dipendente rispetto ai topi mdx-LR.

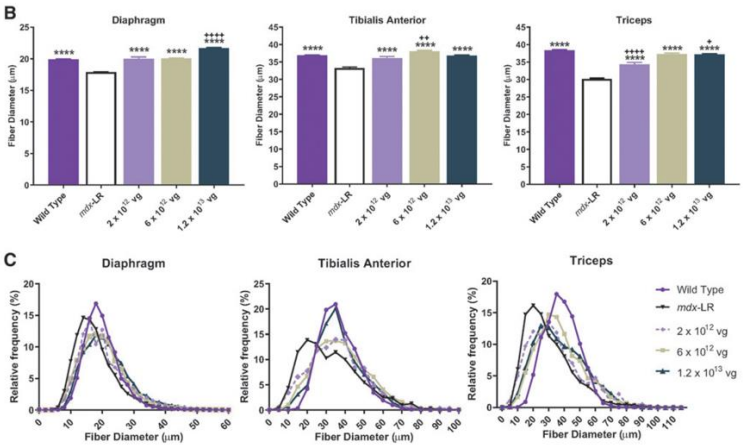

Figura 3.2
(B, C) La quantificazione della dimensione media delle fibre e percentuale della frequenza relativa nel DIA, nel TA e nel TRI in topo WILD TYPE, mdx-LR e in topi trattati con rAAVrh74.MHCK7.micro-distrofina alla dose totale di 2 × 10 ^{12} vg, 6 × 10 ^{12} vg e 1,2 × 10 ^{13} vg.

Al fine di valutare come il trasferimento genico influisse sulla fibrosi, è stata anche valutata la quantità di deposizione di collagene nel muscolo scheletrico, tramite colorazione Picrosirius (Figura 3.3, A).

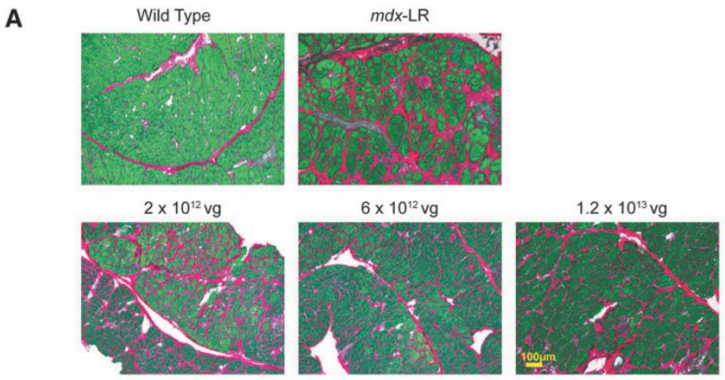

Figura 3.3
(A) Colorazione Picrosirius di DIA in topi wild type, topi mdx -LR e topi mdx trattati con rAAV74.MHCK7.micro-distrofina

Sebbene non ci siano stati cambiamenti significativi tra la dose più alta e il wild type, il trasferimento genico con rAAVrh74.MHCK7.micro-distrofina ha ridotto la deposizione di collagene nel DIA (Figura 3.3, B), seguita da un notevole aumento della forza di uscita del DIA a valori paragonabili a quelli osservati negli animali wild type. (Figura 3.3, C)

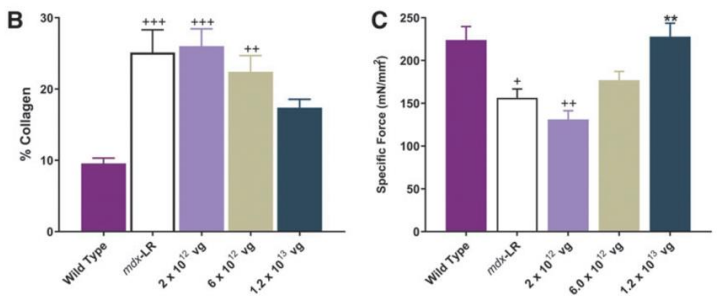

Figura 3.3
(B) Percentuale di collagene nel DIA dei topi wild type, mdx-topi LR e topi mdx trattati con rAAVrh74.MHCK7.micro-distrofina.
(C) Media della forza specifica rilevata nel DIA in topi wild type, topi mdx -LR e topi mdx trattati con rAAVrh74.MHCK7.micro-distrofina.

- **Miglioramenti funzionali con somministrazione sistemica in modo dose-dipendente**

Sono state valutate le caratteristiche dei muscoli DIA e TA di topi wild type, mdx-LR e topi trattati con rAAVrh74.MHCK7.micro-distrofina ai tre livelli di dose, per stabilire se Il trasferimento del gene della micro-distrofina offrisse un vantaggio funzionale al muscolo malato.

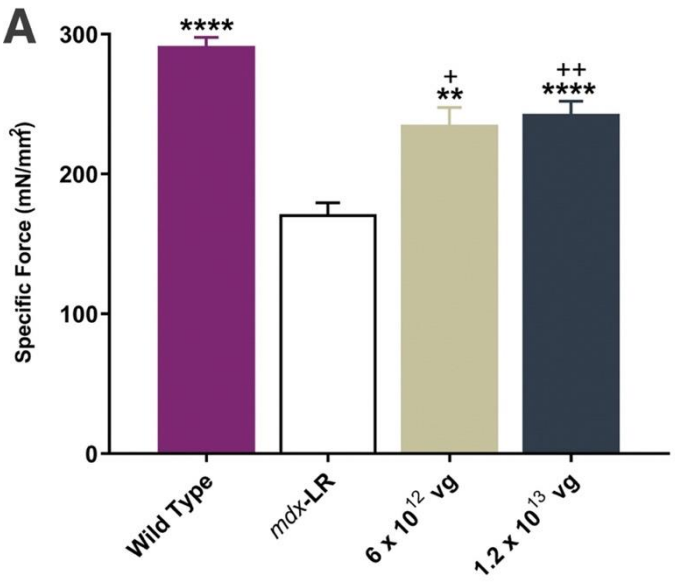

Figura 3.4

(A) Forza specifica misurata nel muscolo DIA.

La forza specifica nel DIA è aumentata gradualmente dopo la somministrazione nella vena caudale di rAAVrh74.MHCK7.micro-distrofina (176,9 mN/mm^2 nel gruppo a dose intermedia contro 227,78 mN/mm^2 nel gruppo ad alto dosaggio), raggiungendo livelli paragonabili a quelli del wild type (Figura 3.4, A).

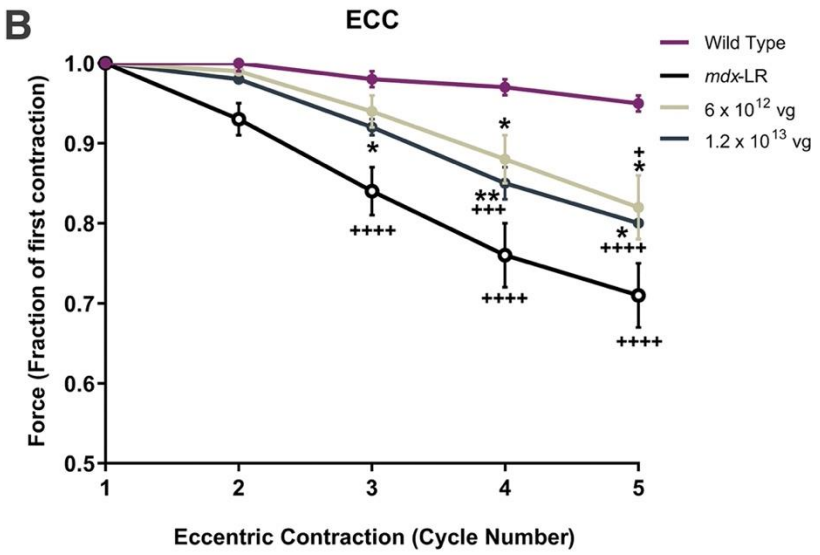

Figura 3.4
(B) Perdita di forza nel muscolo TA valutata utilizzando un rigoroso protocollo ECC. La forza in uscita viene tracciata ad ogni ciclo (media del lato sinistro e destro per animale, per coorte

Inoltre, è stato dimostrato che i topi mdx-LR presentavano carenze funzionali nel muscolo TA rispetto ai topi wild type, come evidenziato da un calo del 58% nella produzione di forza (171,3 vs 291,65 mN/mm^2) e una maggiore perdita di forza a seguito di contrazioni eccentriche (perdita del 32% negli animali mdx-LR).
Dopo aver eseguito un impegnativo esercizio di contrazione eccentrica, in topi trattati con rAAVrh74.MHCK7.micro-distrofina la capacità dei muscoli AT di produrre forza è migliorato in modo significativo (Figura 3.4, B) e li ha protetti dai danni causati dalla contrazione. Nei muscoli TA e DIA di topi in cui era stata somministrato il costrutto rAAVrh74.MHCK7.micro-distrofina è stata osservata una maggiore generazione di forza.
Inoltre, un calo del 75% della creatina chinasi dimostrato che la micro-distrofina difende significativamente le membrane muscolari dai danni (Figura 3.4, C).

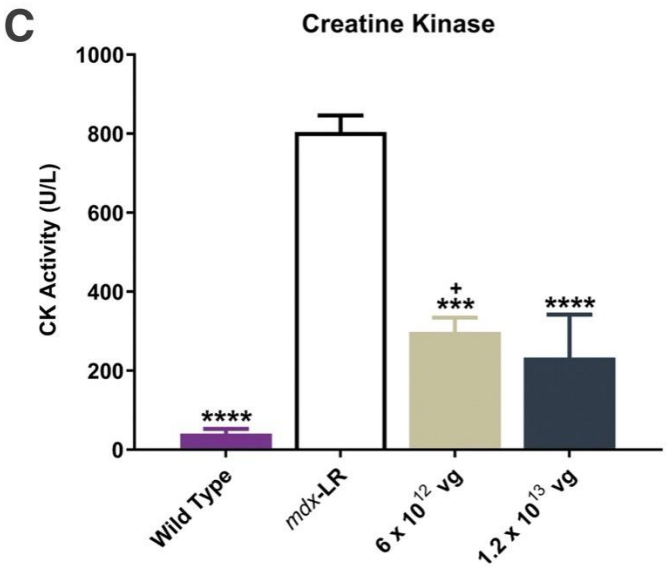

Figura 3.4

(C) Livelli sierici di CK tre mesi dopo il trattamento

È stata poi svolta l'analisi Western blot per valutare altri componenti associati al complesso DGC, come l'enzima nNOS (Figura 3.5, A).

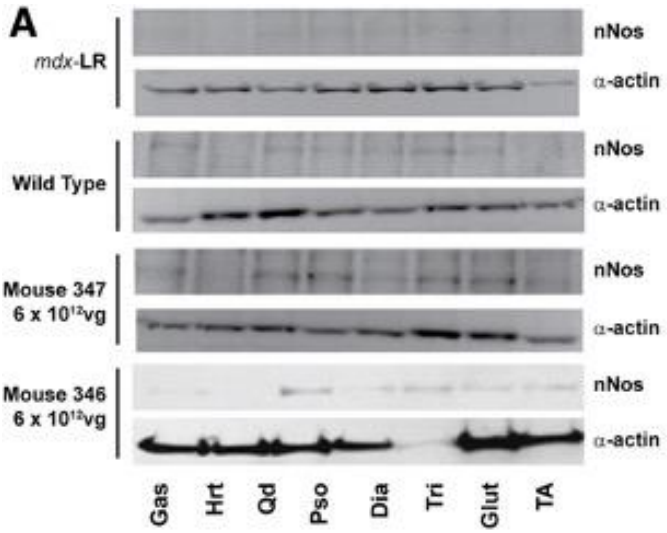

Figura 3.5

(A) Analisi Western blot; l'α-actinina è stata utilizzata come controllo di caricamento

Nonostante la micro-distrofina non contenga le ripetizioni 16 e 17 al livello del dominio centrale (sito di legame per nNOS nel sarcolemma), durante l'esame dell'espressione della proteina nNOS mediante Western blot per tutti i muscoli esaminati negli animali trattati la quantità di proteina nNOS nel muscolo scheletrico è uguale alla quantità trovata nei tessuti wild type TA e aumentata rispetto al topo mdx non trattato.

- **Biodistribuzione del vettore dopo la consegna sistemica**

Utilizzando qPCR in tempo reale è stato possibile rilevare la trascrizione di rAAVrh74.MHCK7.micro-distrofina a livelli variabili in base al tessuto analizzato.
Per esempio, i livelli più alti sono stati osservati nel muscolo scheletrico e nel cuore e negli organi di eliminazione mentre i livelli più bassi sono stati rilevati in gonadi, polmoni e reni (Figura 3.5, B).

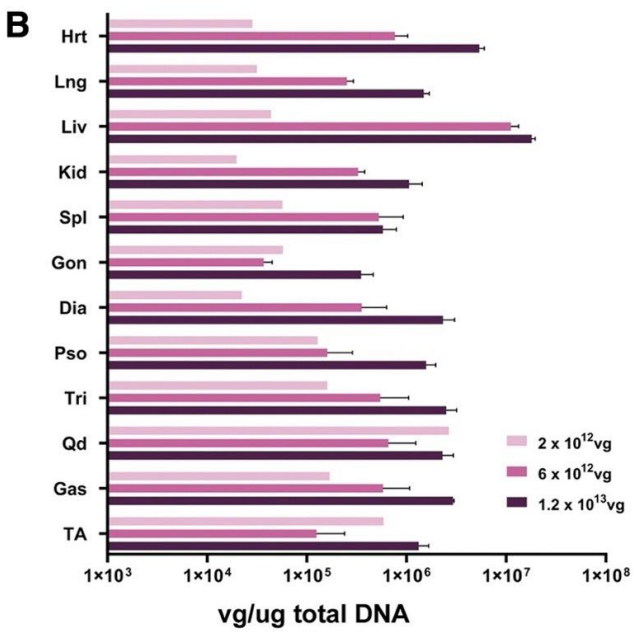

Figura 3.5 *(B) Biodistribuzione di vgs normalizzata a microgrammi di DNA in organi e tessuti dopo la consegna sistemica di rAAVrh74.MHCK7.micro-distrofina.*

Per mezzo del Western blot è stato possibile osservare la presenza della micro-distrofina in tutti i muscoli scheletrici analizzati (Figura 3.5, C), con la quantità più alta nel cuore nei tessuti dei topi trattati con dosi intermedie e alte, mentre non è stata rilevata in nessun organo fuori bersaglio (solo una debole banda è stata osservata nel fegato alla dose più alta, che potrebbe essere al limite inferiore di rilevamento).

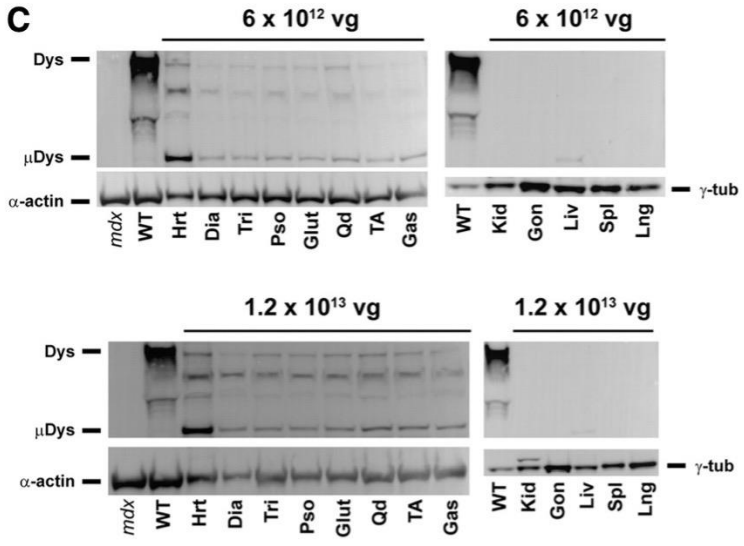

Figura 3.5 *(C) Analisi Western blot; l'α-actinina e laγ-tubulina sono state utilizzate come controllo di caricamento*

Infine, non sono stati osservati effetti istopatologici avversi nel fegato e nessuna chimica del sangue anormale in nessuna delle coorti dosate.

- **Miglioramenti duraturi dopo una singola infusione sistemica**

Per valutare l'espressione a lungo termine e il beneficio funzionale di una singola somministrazione endovenosa di rAAVrh74.MHCK7.micro-distrofina, una coorte di topi maschi mdx è stata iniettata con una dose intermedia (6 x 10^{12} vg) a 4 settimane di età e sottoposta a necroscopia a 6 mesi dopo l'iniezione. Il muscolo scheletrico (TA), il cuore e il DIA sono stati colorati con un anticorpo distrofina N-terminale per rilevare l'espressione del transgene micro-distrofina (Figura 3.6, A). L'istologia è stata analizzata mediante colorazione con ematossilina ed eosina (Figura 3.6, B).

Oltre alla DIA di tutti gli animali trattati, sei muscoli scheletrici (TA, GAS, QD, PSO, TRI, GLUT) sono stati analizzati tramite immunofluorescenza per valutare l'espressione del transgene della micro-distrofina.

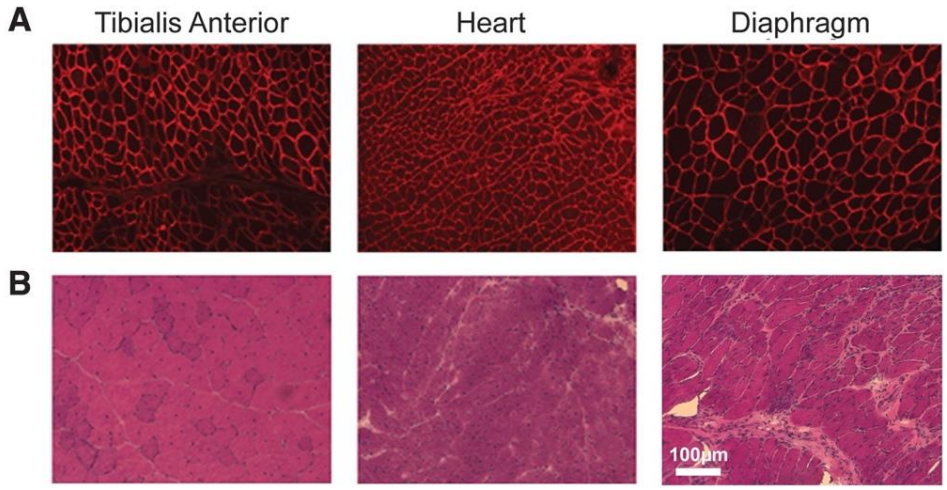

Figura 3.6 *(A)Colorazione immunofluorescente rappresentativa per micro-distrofina utilizzando un anticorpo distrofina N-terminale e TA, cuore. (B) DIA colorati con ematossilina ed eosina di topi mdx trattati con rAAVrh74.micro-distrofina a un livello intermedio (6 × 10 [12] vg) dose, 6 mesi dopo il trattamento*

Nel muscolo AT, la somministrazione sistemica di una dose intermedia (6 x 10^{12} vg) di rAAVrh74.MHCK7.micro-distrofina ha determinato la localizzazione del 65,5% delle fibre con micro-distrofina alla membrana, ha migliorato l'uscita della forza specifica a 235,4 mN/mm^2, e ha protetto il muscolo dai danni causati da ripetute contrazioni eccentriche con una diminuita forza del 25% (Figura 3.6, C-D).

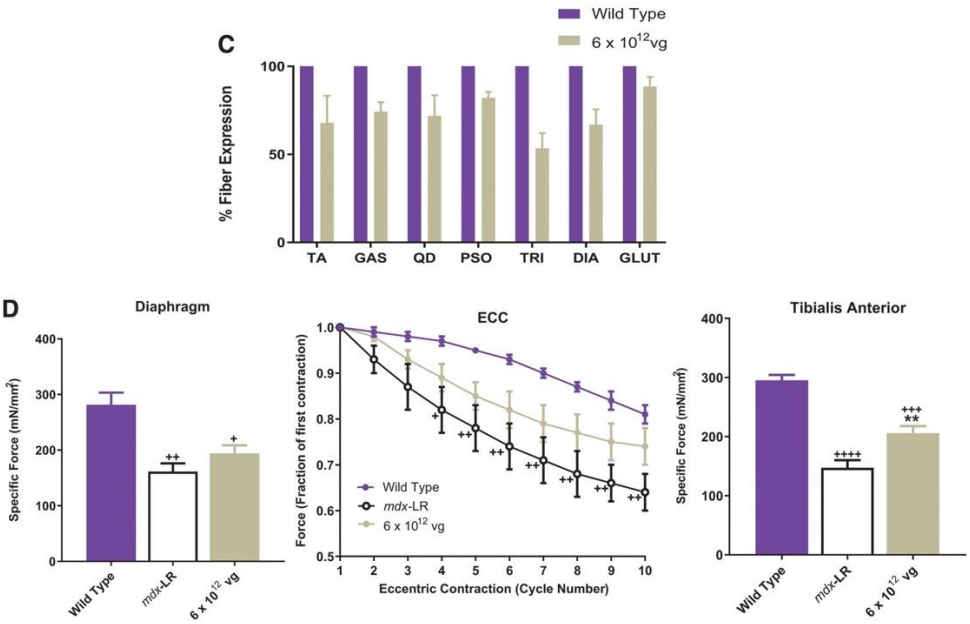

Figura 3.6 *(C) Percentuale di fibre positive all'immunofluorescenza che esprimono la proteina micro-distrofina 6 mesi dopo un singolo trattamento con. (D) Generazione di forza specifica nei muscoli DIA e AT 6 mesi dopo un trattamento; Perdita di forza eccentrica secondo un rigoroso protocollo ECC*

Questi risultati mostrano che l'espressione transgenica è stata preservata sei mesi dopo l'iniezione e che i vantaggi funzionali visti in precedenza sia nel DIA che nell'AT non sono diminuiti, indicando effetti prolungati (durata a lungo termine) dopo un singolo trattamento.

○ DISCUSSIONE

Questo studio si basa sulla progettazione di una cassetta terapeutica di micro-distrofina umana, la quale presenta un doppio promotore specifico del muscolo striato grazie al quale si ha l'espressione selettiva del transgene nel muscolo scheletrico e cardiaco. Il gene di micro-distrofina è stato confezionato in un vettore rAAVrh74, sierotipo isolato dai linfonodi delle scimmie rhesus, il quale ha mostrato un'elevata affinità per il tessuto muscolare scheletrico e cardiaco e una robusta potenza nella biodistribuzione, consegna e trasduzione di varie proteine. La sieroprevalenza è bassa.

Ciò che rende efficace e sicura una terapia genica AAV, oltre alla consegna del vettore, è la regolazione dell'espressione del transgene nel tessuto bersaglio, in questo caso il muscolo scheletrico e cardiaco. Per ottenere la massima espressione genica nei tessuti target, limitando allo stesso tempo l'espressione nei tessuti out of target, in questo studio è stato utilizzato MHCK7, che, come precedentemente affermato, presenta un potenziatore α-MHC, utile per ottenere una maggiore espressione nei cardiomiociti, aumentando allo stesso tempo l'espressione di

distrofina nel muscolo scheletrico. La biodistribuzione in questo studio ha infatti sottolineato la limitata espressione out of target del transgene, consentendo l'espressione stessa solo nei tessuti target quali muscolo scheletrico e cardiaco.
La somministrazione sistemica di rAAVrh74.MHCK7.micro-distrofina ha mostrato un miglioramento nella generazione di forza di DIA e TA, diminuzione dell'infiammazione e delle caratteristiche distrofiche sia a dosi intermedie che alte. Non c'era alcuna differenza distinguibile nei livelli di degenerazione e nella diminuzione dell'infiammazione tra i due gruppi di dosaggio, ma la riduzione dell'istopatologia distrofica era più pronunciata in queste due coorti rispetto alla dose inferiore. Le coorti a maggior dosaggio hanno mostrato una miopatia significativamente inferiore nel cuore e in tutti gli altri tessuti.
Il DIA ha rivelato i cambiamenti più marcati nelle coorti dosate.
Le coorti trattate con il vettore avevano una miopatia sostanzialmente ridotta in tutti i tessuti e nel cuore. Di interesse, i livelli sierici di CK erano significativamente ridotti nei topi mdx dopo il trattamento con rAAVrh74.MHCK7.micro-distrofina, rispetto ai topi mdx-LR.
L'aumento della concentrazione di nNOS nei muscoli scheletrici rispetto ai topi mdx-LR può suggerire che la presenza di questa proteina, e non la sua localizzazione specifica nel muscolo, sia essenziale per la funzionalità del muscolo.
Oltre all'efficacia, questo studio di aumento della dose ha dimostrato una tossicità minima quando i topi sono stati trattati con rAAVrh74.MHCK7.micro-distrofina anche alla dose totale più alta di $1{,}2 \times 10^{13}$ vg.
La domanda che ci si pone ore è se il trasferimento di rAAVrh74.MHCK7.micro-distrofina è sicuro e ben tollerato nei pazienti con distrofia muscolare di Duchenne. Ad oggi si stanno svolgendo vari studi su pazienti con distrofia muscolare che stanno rispondendo positivamente al trattamento.

4. BIBLIOGRAFIA

Chang NC, Chevalier FP, Rudnicki MA.
Satellite Cells in Muscular Dystrophy - Lost in Polarity.
Trends Mol Med. 2016 Jun;22(6):479-496.

Duan, D., Goemans, N., Takeda, S. *et al.*
Duchenne muscular dystrophy.
Nat Rev Dis Primers **7**, 13 (2021).

Giovarelli M, Arnaboldi F, Zecchini S, Cornaghi LB, Nava A, Sommariva M, Clementi EGI, Gagliano N.
Characterisation of Progressive Skeletal Muscle Fibrosis in the Mdx Mouse Model of Duchenne Muscular Dystrophy: An In Vivo and In Vitro Study.
Int J Mol Sci. 2022 Aug 5;23(15):8735.

Hakim CH, Li D, Duan D.
Monitoring murine skeletal muscle function for muscle gene therapy.
Methods Mol Biol. 2011;709:75-89.

Harper, S., Hauser, M., DelloRusso, C. *et al.*
Modular flexibility of dystrophin: Implications for gene therapy of Duchenne muscular dystrophy.
Nat Med **8**, 253–261 (2002).

Manini A, Abati E, Nuredini A, Corti S, Comi GP.
Adeno-Associated Virus (AAV)-Mediated Gene Therapy for Duchenne Muscular Dystrophy: The Issue of Transgene Persistence.
Front Neurol. 2022 Jan 5;12:814174.

Moorwood C, Liu M, Tian Z, Barton ER.
Isometric and eccentric force generation assessment of skeletal muscles isolated from murine models of muscular dystrophies.
J Vis Exp. 2013 Jan 31;(71):e50036.

Salva MZ, Himeda CL, Tai PW, Nishiuchi E, Gregorevic P, Allen JM, Finn EE, Nguyen QG, Blankinship MJ, Meuse L, Chamberlain JS, Hauschka SD.
Design of tissue-specific regulatory cassettes for high-level rAAV-mediated expression in skeletal and cardiac muscle.
Mol Ther. 2007 Feb;15(2):320-9.

RESEARCH ARTICLES

HGT

Dose-Escalation Study of Systemically Delivered rAAVrh74.MHCK7.micro-dystrophin in the *mdx* Mouse Model of Duchenne Muscular Dystrophy

Rachael A. Potter,[1,2] Danielle A. Griffin,[1,2] Kristin N. Heller,[2] Ellyn L. Peterson,[1,2] Emma K. Clark,[2] Jerry R. Mendell,[2,3] and Louise R. Rodino-Klapac[1–3]

[1]*Sarepta Therapeutics, Inc., Cambridge, Massachusetts, USA.*
[2]*Center for Gene Therapy, The Research Institute at Nationwide Children's Hospital, Columbus, Ohio, USA.*
[3]*Department of Pediatrics and Neurology, The Ohio State University, Columbus, Ohio, USA.*

Duchenne muscular dystrophy (DMD) is a rare, X-linked, fatal, degenerative neuromuscular disease caused by mutations in the *DMD* gene. More than 2,000 mutations of the *DMD* gene are responsible for progressive loss of muscle strength, loss of ambulation, and generally respiratory and cardiac failure by age 30. Recently, gene transfer therapy has received widespread interest as a disease-modifying treatment for all patients with DMD. We designed an adeno-associated virus vector (rAAVrh74) containing a codon-optimized human micro-dystrophin transgene driven by a skeletal and cardiac muscle-specific promoter, MHCK7. To test the efficacy of rAAVrh74.MHCK7.micro-dystrophin, we evaluated systemic injections in *mdx* (dystrophin-null) mice at low (2×10^{12} vector genome [vg] total dose, 8×10^{13} vg/kg), intermediate (6×10^{12} vg total dose, 2×10^{14} vg/kg), and high doses (1.2×10^{13} vg total dose, 6×10^{14} vg/kg). Three months posttreatment, specific force increased in the diaphragm (DIA) and tibialis anterior muscle, with intermediate and high doses eliciting force outputs at wild-type (WT) levels. Histological improvement included reductions in fibrosis and normalization of myofiber size, specifically in the DIA, where results for low and intermediate doses were not significantly different from the WT. Significant reduction in central nucleation was also observed, although complete normalization to WT was not seen. No vector-associated toxicity was reported either by clinical or organ-specific laboratory assessments or following formal histopathology. The findings in this preclinical study provided proof of principle for safety and efficacy of systemic delivery of rAAVrh74.MHCK7.micro-dystrophin at high vector titers, supporting initiation of a Phase I/II safety study in boys with DMD.

Keywords: Duchenne muscular dystrophy, AAV, micro-dystrophin, dose-escalation, gene therapy, rAAVrh74.MHCK7.micro-dystrophin, *mdx* mouse model

INTRODUCTION

DUCHENNE MUSCULAR DYSTROPHY (DMD) is a rare, X-linked, fatal, degenerative neuromuscular disease that occurs in ~1 in every 3,500 to 5,000 males born worldwide.[1–4] DMD and Becker muscular dystrophy (BMD) affect skeletal and cardiac muscle due to mutations in the 2.4 Mb dystrophin gene (*DMD*). Dystrophin is a 427 kDa cytoskeletal protein required for muscle fiber stability. Specifically, dystrophin links the sarcomere and the extracellular matrix. Loss of the protein results in destabilization of the dystrophin-associated protein complex (DAPC), repeated turnover of the muscle, satellite cell depletion, and replacement of fibers by fat and fibrosis. The most frequent mutations (65%) found in patients are deletions of one or more exons of the *DMD* gene, leading to shortened forms of nonfunctional dystrophin protein that undergo degradation.[5] Patients with DMD are characterized by progressive muscle weakness affecting skeletal and respiratory muscle and loss of ambulation typically by age 12, and generally death by age 30.[6]

Corticosteroids are currently the standard-of-care treatment for most patients to modify symptoms.[7] However, while corticosteroids have shown benefit in delaying disease progression, long-term treatment is limited as it is

*Correspondence: Dr. Louise R. Rodino-Klapac, Sarepta Therapeutics, Inc., 215 First Street, Cambridge, MA, 02142, USA. E-mail: lrodinoklapac@sarepta.com

associated with serious adverse effects such as bone fracture, infection, and gastrointestinal bleeding.[8] Moreover, once decline occurs, disease progression remains fatal as dilated cardiomyopathy and respiratory failure are often the major cause of premature death.[6] Eteplirsen is the first disease-modifying treatment (phosphorodiamidate morpholino oligomer) approved in the United States for DMD in patients with confirmed *DMD* mutations amenable to exon 51 skipping.[9–11] Eteplirsen has been shown to produce functional dystrophin protein and slow the decline in ambulatory and pulmonary function after long-term use.[9–12] Golodirsen was the first treatment approved by the U.S. Food and Drug Administration for DMD patients amenable to exon 53 skipping,[13] and a second antisense oligonucleotide has been approved for the same group of patients.[14] Recently there has been a significant focus on developing gene therapy approaches for DMD with the potential to become a disease-modifying treatment for all patients with DMD following single gene delivery.

Adeno-associated virus (AAV) systemic gene transfer therapy offers the possibility to ameliorate disease progression and normalize the muscle environment through restoration of dystrophin expression in cardiac and skeletal muscle. However, due to the enormous size of the dystrophin gene and the packaging limitation of AAV ($\sim$5 kb), entire gene transfer is not feasible. Thus, investigators have developed micro-dystrophin genes that produce shortened functional variants of micro-dystrophin protein and demonstrated amelioration of muscle pathology and cardiomyopathy in various preclinical models.[15–20]

More than 30 different configurations of micro-dystrophin have been developed based upon the genotypes of patients with milder forms of DMD/BMD and preclinical structure–function studies.[21] Dystrophin is composed of four major domains: an N-terminus that contains an actin binding domain, a central rod domain of 24 spectrin repeats (R) that is flanked and interspersed with 4 hinge (H) subdomains, a cysteine-rich domain, and a C-terminal domain.[22–24] The N-terminus and cysteine-rich domain are thought to be essential, as these contain an actin binding site[22] and the binding domain for β-dystroglycan,[25,26] respectively. In contrast, the C-terminus does not appear to be essential for muscle function or DAPC assembly.[23] The central rod domain is the largest and plays an important role in conferring protection and flexibility.[24,27] However, only a few spectrin repeats and hinges have been demonstrated to have functional relevance.[27,28] For example, spectrin repeats R2-3 have been shown to be necessary for optimized resistance to eccentric force loss,[28] and early structural studies have demonstrated that R1-3 may interact with the lipid membrane.[29,30] We have designed a micro-dystrophin transgene that would promote optimized functional efficacy upon delivery.

In addition to the micro-dystrophin transgene sequence, the efficacy and safety of AAV micro-dystrophin gene therapy are also dictated by the promoter sequence. Therefore, to maximize gene expression in cardiac and skeletal muscle, the cassette used for this study includes a skeletal and cardiac muscle-specific promoter, MHCK7, which provides assurance of safety and avoidance of off-target effects.[31,32] This promoter includes an α-myosin heavy chain complex (α-MHC) enhancer that leads to high levels of expression in cardiomyocytes and increased dystrophin expression in skeletal muscle versus MCK or CK7.[32–34] In the present study, a dose-escalation study design was utilized to evaluate safety and efficacy in the *mdx* mouse model of DMD. This report provides proof of principle for the efficacy and safety of systemic delivery of rAAVrh74.MHCK7.micro-dystrophin vector in an *mdx* mouse model of DMD at 3 and 6 months post-transgene delivery and supports initiation of a Phase I/II safety study in boys with DMD.

MATERIALS AND METHODS

Animal models

Dystrophin-deficient mouse strain. All procedures were approved by The Research Institute at Nationwide Children's Hospital Institutional Animal Care and Use Committee (protocol AR08-00009; AR06-00054). Stocks of C57BL/6 and C57BL/10ScSn-Dmd^{mdx}/J mice were bred and maintained as homozygous animals in standardized conditions in the Animal Resources Core at The Research Institute at Nationwide Children's Hospital. Mice were maintained on Teklad Global Rodent Diet (3.8% fiber, 18.8% protein, 5% fat chow) with a 12-h dark/12-h light cycle. All mice used in this study were male.

Micro-dystrophin gene construction

For all gene transfer studies, the human micro-dystrophin cassette contained the (R4–R23/Δ71–78) domains as previously described.[35] The complementary DNA was codon optimized for human usage and synthesized by GenScript (Piscataway, NJ). It includes a consensus Kozak sequence, an SV40 intron, and synthetic polyadenylation site (53 base pairs). The recombinant MHCK7 promoter used to drive transgene expression is a dual striated muscle-specific promoter and is based on the MCK promoter and the promoter described by Dr. Stephen Hauschka (University of Washington, Seattle, WA).[32] This MCK-based promoter utilizes an enhancer derived from the 5′ of the transcription start site within the endogenous muscle CK gene with a proximal promoter.[32] This enhancer, along with a modified CK7 cassette from the MCK family of genes, is ligated to an α-MHC enhancer 5′ of the CK portion to promote cardiac expression.[32] The MHCK7 micro-dystrophin expression cassette was cloned between AAV2 inverted terminal repeats (ITRs) using

flanking *Xba*I restriction enzyme sites. *Msc*I/*Sma*I restriction enzyme digestions, as well as Sanger sequencing through the ITRs, were used to confirm ITR integrity.

AAV vector production

rAAVrh74.MHCK7.micro-dystrophin was packaged into AAV serotype rh74 capsid using the standard triple transfection protocol as previously described.[31,36,37] A quantitative polymerase chain reaction (qPCR)-based titration method was used to determine an encapsulated vector genome (vg) titer utilizing a Prism 7500 Fast TaqMan detector system (PE Applied Biosystems).[38]

In vivo gene delivery

The mice in this study were randomized in sequential order and dosed per mean body weight per group. *Mdx* mice were injected in the tail vein at 4 to 5 weeks of age with Lactated Ringer (LR) solution (untreated, *mdx*-LR, $n=6$) or with rAAVrh74.MHCK7.micro-dystrophin at escalating doses: 2×10^{12} vg total dose, 8×10^{13} vg/kg ($n=5$); 6×10^{12} vg total dose, 2×10^{14} vg/kg ($n=8$); or 1.2×10^{13} vg total dose, 6×10^{14} vg/kg ($n=8$). Each cohort of mice was necropsied at 12 weeks postvector delivery for histological, functional, and expression analysis. A separate cohort of mice, also injected at 4 to 5 weeks of age with the intermediate dose (6×10^{12} vg) ($n=8$), was necropsied at 24 weeks postvector delivery for long-term analysis of histological, functional, and expression outcome measures. All data acquisition and analysis were blinded to treatment group.

Hematology

Whole blood was obtained from cardiac puncture for serum chemistry panel analysis for C57BL/6 wild-type (WT), *mdx*-LR, intermediate dose (6×10^{12} vg) and high dose (1.2×10^{13} vg). Blood was collected into a serum separating tube and centrifuged for 10 min at 15,000 rpm. Supernatant was collected, frozen, and sent to Charles River Laboratories for chemistry testing. Due to limited sample volume, liver enzymes and glucose chemistries were prioritized.

Histopathology

Following euthanization, necropsy was performed, and organ samples were collected. Muscle tissue was fresh frozen in liquid nitrogen-cooled methylbutane, and all other organs were harvested, fixed in formalin, and embedded in paraffin. After processing, tissues were stained with hematoxylin and eosin, and slides and all tissues were sent to GEMPath, Inc., for blinded histopathology evaluation by a veterinary pathologist. The pathologist was subsequently unblinded for data analysis and report development.

Diaphragm tetanic contraction for functional assessment

Mice were euthanized, and the diaphragm (DIA) was dissected with rib attachments and central tendon intact and placed in Kreb's–Henseleit (K-H) buffer as previously described.[39–43] One 2–4 mm wide section of DIA was isolated per animal per cohort (for one animal in the intermediate dose, two strips were analyzed). DIA strips were tied firmly with braided surgical silk (4-0; Surgical Specialties, Reading, PA) at the central tendon and sutured through a portion of rib bone affixed to the distal end of the strip. Each muscle was transferred to a water bath filled with oxygenated K-H solution that was maintained at 37°C. The muscles were aligned horizontally and tied directly between a fixed pin and a dual-mode force transducer-servomotor (305C; Aurora Scientific, Aurora, Ontario, Canada). Two platinum plate electrodes were positioned in the organ bath, to flank the length of the muscle. The muscle was stretched to an optimal resting tension of 1 g force (the current was set to 1A for duration of the analysis). The muscle was then allowed to rest for 5 min before initiation of the tetanic protocol.

Once the muscle was stabilized, it was subjected to a warm-up, which consisted of three 1-Hz twitches every 30 s, followed by three 150-Hz twitches every minute. After a 3-min rest period, the DIA was stimulated at 20, 50, 80, 120, 150, and 180 Hz, allowing a 2-min rest period between each stimulus, each with a duration of 250 ms to determine maximum tetanic force. Muscle length and weight were measured to determine cross-sectional area. The specific force was normalized to the cross-sectional area of the muscle.

Tibialis anterior tetanic contraction for functional assessment

The tibialis anterior (TA) procedure followed the protocol listed in Hakim *et al.*[44] Mice were anesthetized using a ketamine/xylazine mixture. A double square knot was tied around the patellar tendon with a 4-0 suture. The TA distal tendon was then dissected out, a double square knot was tied around the tendon with 4-0 suture as close to the muscle as possible, and then the tendon was cut. The exposed muscle was constantly dampened with saline. Mice were then transferred to a thermal-controlled platform and maintained at 37°C. The knee was secured by placing a metal pin behind the patellar tendon. The suture attached to the distal TA tendon was pulled to a resting tension of 3 g and adjusted to be level with the arm of the force transducer (Aurora Scientific, Aurora, Canada). An electrode was placed near the sciatic nerve to stimulate it.

Once the muscle was stabilized, the resting tension was set to a force (optimal length) where twitch contractions were maximal. To determine the optimal length resting tension was set at 2, 3, 4, 5, and 6 g force and stimulated at 1 Hz to determine the optimal tension to be used throughout the procedure protocol (the current was set to 200 mA for duration of the analysis). After a 3-min rest period, the TA was stimulated at 50, 100, 150, and 200 Hz, allowing a 1-min rest between each stimulus. Following a

5-min rest, the muscles were then subjected to a series of 10 isometric contractions, occurring at 1-min intervals with a 10% stretch–relengthening procedure. After the eccentric contractions, the mice were euthanized, and the TA muscle was dissected out and frozen for histology.

Immunofluorescence

Cryosections (12 μm) from the TA, gastrocnemius (GAS), quadriceps (QD), psoas major (PSO), gluteus (GLUT), triceps (TRI), and DIA muscles along with the heart were subjected to immunofluorescent staining for the dystrophin transgene through our previously used protocol.[39] Sections were incubated with a mouse monoclonal human dystrophin primary antibody (Santa Cruz Biotechnology, Dallas, TX) at a dilution of 1:50 and the human β-sarcoglycan primary antibody (Leica Biosystems, Buffalo Grove, IL) at a dilution of 1:100. Additional detail about antibodies used for immunofluorescence analysis is shown in Supplementary Table S1. Analysis for percentage of fibers positive for dystrophin staining included 4 random 20X images covering the four different quadrants of the muscle section per animal per tissue ($n=5$ per cohort). Images were taken using a Zeiss AxioCam MRC5 camera (Germany). Percentage of fibers positive for dystrophin staining (>50% of muscle membrane staining) was determined for each image. Quantification data of immunofluorescent-positive fibers expressing dystrophin protein are reported as mean ± standard error of the mean of $n=5$ per treatment group.

Western blot analysis

Western blots were performed according to our previously used protocol, with several modifications specific for each antibody used.[39] Samples from WT mice, *mdx*-LR mice, and vector-dosed *mdx* mice were used for each western blot. Protein (50 μg for muscle and organs) extracted from samples was separated by sodium dodecyl sulfate–polyacrylamide gel electrophoresis (SDS-PAGE) (3–8% Novex NuPAGE gradient gels, Invitrogen, Waltham, MA), blotted on polyvinylidene fluoride membrane, and probed with dystrophin primary antibody Dys1 for dystrophin detection and Dys3 for micro-dystrophin (Leica Biosystems) at a dilution of 1:50 and 1:20, respectively, or neuronal nitric oxide synthase (nNOS) primary antibody (Fisher Scientific) at a dilution of 1:1,000. Loading controls used included γ-tubulin antibody (Sigma) or α-actinin antibody (Sigma) at a dilution of 1:10,000 followed by Alexa Fluor 680 goat anti-mouse (1:5,000, LI-COR, Lincoln, Nebraska). Additional detail about antibodies used for western blot analysis is shown in Supplementary Table S1.

Morphometric analysis

Hematoxylin and eosin staining was performed on 12-μm cryosections of muscle from WT mice, *mdx*-LR mice, and rAAVrh74.MHCK7.micro-dystrophin-treated *mdx* mice for analysis. Muscle fiber diameters were measured using minimal Feret's diameter in all muscles. Analysis for fiber diameters included 4 fields of 20X magnification per animal per side per tissue (low dose, $n=4$; intermediate and high dose, $n=8$; *mdx*-LR and WT, $n=6$). There was a range of 1,000–5,000 fibers quantified per muscle from each treatment group and control cohorts. In addition, the percentage of myofibers with central nuclei was determined analyzing four fields of 20X image magnification per animal from the left side for TA, GAS, QD, PSO, GLUT, TRI, and DIA muscles (low dose, $n=5$; intermediate dose, $n=6$; and high dose, $n=7$; *mdx*-LR and WT, $n=6$). Images were taken with a Zeiss AxioCam MRC5 camera. Fiber diameters were measured using Zeiss AxioVision LE4 software, and centrally nucleated fibers were quantified using the National Institutes of Health ImageJ software.

Biodistribution qPCR analysis

TaqMan qPCR was performed to quantify the number of vg copies present in targeted muscle, as well as nontargeted organs, as previously described.[34,45,46] Biodistribution analysis was performed on tissue samples collected from three vector-dosed *mdx* animals per dose level. Tissues were harvested at necropsy, and vector-specific primer probe sets specific for sequences of the MHCK7 promoter were utilized. A vector-specific primer probe set was used to amplify a sequence of the intronic region directly downstream from the MHCK7 promoter that is unique and located within the rAAVrh74.MHCK7.micro-dystrophin transgene cassette. A positive signal was defined as anything ≥100 single-stranded DNA copies/μg genomic DNA detected. Copy number is reported as vg/μg genomic DNA.

Picrosirius red stain and collagen quantification

Frozen sections placed onto Fisherbrand Superfrost charged microscope slides were fixed in 10% neutral buffered formalin for 5 min and then rinsed in distilled water. Slides were then incubated in Solution B (Direct Red 80/2 4 6-Trinitrophenol) from the Picrosirius Red Stain Kit (Polysciences, Inc., Mount Arlington, NJ, Catalog no. 24901) for 15 min. After a thorough rinse in distilled water, the slides were placed in Solution C (0.1 N hydrochloride acid) for 2 min. Slides were counterstained for 5 min with 1% Fast Green in 1% glacial acetic acid from Poly Scientific (Bay Shore, NY, Catalog no. S2114) using a 1:10 dilution in deionized water. Finally, the slides were rinsed again in distilled water, dehydrated in graded ethanol, cleared in xylene, and mounted with coverslips using Cytoseal 60 media from Thermo Scientific (Catalog no. 8310). Images were taken using the AxioVision 4.9.1 software. Representative images of DIA tissue sections in *mdx* mice treated with rAAVrh74.MHCK7.micro-dystrophin were compared to *mdx*-LR mice at 20X magnification.

For analysis of Sirius red staining and percent collagen quantification, the contrast between the red and the green colors was enhanced using Adobe Photoshop. The color deconvolution plugin in the ImageJ software program was selected, and the RGB color deconvolution option was used. The red image includes all connective tissue from the Sirius red stain. The green image includes all muscle from the Fast Green counterstain. Only the red image and the original image were used. A threshold was applied to the images to obtain black and white images with areas positive for collagen in black and negative areas in white. Using the measure function, the area of collagen was calculated. The total tissue area was determined by converting the original image to ''8-bit'' and adjusting the threshold to 254 (one unit below completely saturating the image). The total tissue area was measured as done previously, and total area was recorded. Quantification of collagen accumulation in the DIA of WT mice, *mdx*-LR, and mice treated with low (2×10^{12} vg), intermediate (6×10^{12} vg), and high (1.2×10^{13} vg) doses was calculated by dividing the area of collagen by total tissue area and used to determine the mean percentage for each individual ($n=5$, low dose; $n=8$, intermediate and high dose; $n=6$, *mdx*-LR; and $n=5$, WT).

Statistical analysis

Data are expressed as the mean ± standard error of the mean (SEM; error bars) and were analyzed using a one-way analysis of variance (ANOVA) or two-way ANOVA with multiple comparisons between groups and statistical significance determined through Tukey's *post hoc* analysis test using GraphPad Prism 5 (GraphPad Software, La Jolla, CA), unless otherwise specified.

RESULTS

Our micro-dystrophin transgene cassette was constructed by replacing the MCK promoter from previous studies with the MHCK7 promoter to enhance cardiac expression.[34] To establish the minimal efficacious dose *in vivo*, a dose-escalation study was performed. The dosing groups included a low dose of 2×10^{12} vg total, intermediate dose of 6×10^{12} vg total, and high dose of 1.2×10^{13} vg total. These doses were kept consistent throughout the study, and efficacy was determined through systemic delivery to the tail vein of *mdx* mice.

Histological improvements with systemic delivery in a dose-dependent manner

Four- to five-week-old *mdx* mice were treated with low, intermediate, or high total dose of rAAVrh74.MHCK7.micro-dystrophin intravenously in the tail vein. Mice were necropsied 3 months postinjection, and micro-dystrophin transgene expression was demonstrated using immunofluorescent staining in both the left and right side skeletal muscles, including TA, GAS, QD, PSO, TRI, and GLUT. In addition, the DIA and heart were analyzed. Immunofluorescent staining showed robust micro-dystrophin expression at the sarcolemma membrane of skeletal and cardiac muscle after systemic delivery of rAAVrh74.MHCK7.microdystrophin; representative immunohistochemistry images are shown at the intermediate dose (6×10^{12} vg total) in Fig. 1A and Supplementary Fig. S1. Micro-dystrophin expression levels in each individual muscle type were averaged from all treated mice. The mean percentage expression of micro-dystrophin positive fibers in treated mice was $46.7\%\pm8.08\%$, $66.8\%\pm6.18\%$, and $78.3\%\pm4.7\%$ for low, intermediate, and high dose, respectively, across all muscles (data represented as mean ± SEM, Fig. 1B). For all doses we observed high-level expression in the heart, with intermediate and high dose resembling WT expression levels in all animals (Fig. 1A and Supplementary Fig. S1). Importantly, the variation of micro-dystrophin positive fiber expression across each animal per cohort ($n=5$) in each tissue was not statistically different within dosing cohorts (less than 10% difference). We also assessed the restoration of additional DAPC components in skeletal muscle (*e.g.*, TA) following micro-dystrophin gene transfer and found restoration of β-sarcoglycan in addition to dystrophin expression (Fig. 1A).

Fibrosis and inflammation have been previously reported in *mdx* muscle as part of the chronic dystrophic process. Therefore, fiber diameter, fibrosis, and central nucleation (CN) were evaluated postinjection to evaluate the muscle environment postvector delivery compared to *mdx*-LR mice. Gene transfer significantly reduced pathological severity at intermediate and high vector doses administered. Furthermore, gene transfer showed reduction of dystrophic features, including fibrosis (Fig. 2A and Supplementary Fig. S2A), and normalization of fiber size distribution with a significant increase in fiber diameter, indicating fiber size similar to WT fibers, specifically in the DIA, where results for low and intermediate doses were not significantly different from the WT. We also observed a normalization of fiber size in the TA for low and high doses and at the intermediate dose for the TRI (Fig. 2B and Supplementary Fig. S2B). Quantification of histological parameters demonstrated a significant reduction in CN in all skeletal muscles analyzed in a dose-dependent manner compared to *mdx*-LR mice. Gene transfer did not result in complete normalization to WT, and CN remains significantly higher in treated animals but we observed a significant improvement in the TA and GAS of the high dose cohort (Supplementary Fig. S2C).

In addition, Sirius red quantification, which represents the amount of collagen deposition in skeletal muscle, was measured to assess the effect of gene transfer on fibrosis (Fig. 3A). Gene transfer with rAAVrh74.MHCK7.micro-dystrophin decreased collagen deposition in the DIA, showing an

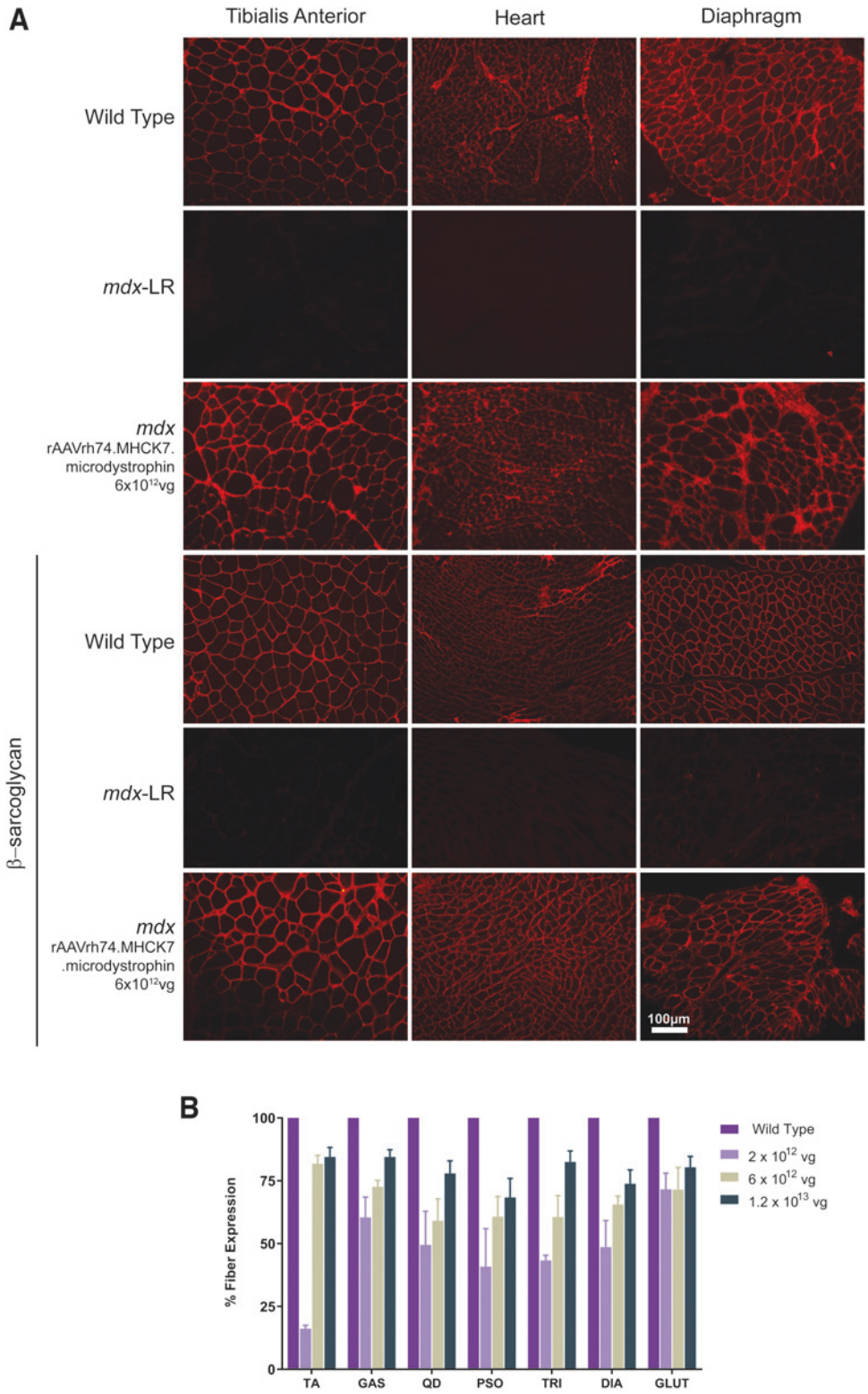

Figure 1. Robust micro-dystrophin expression at the sarcolemma membrane of skeletal and cardiac muscle after systemic delivery of rAAVrh74.MHCK7.micro-dystrophin. Mice received rAAVrh74.MHCK7.micro-dystrophin intravenously at 2.0×10^{12} vector genome (vg) total (low), 6×10^{12} vg total (intermediate), and 1.2×10^{13} vg total (high) dose. **(A)** Representative immunohistochemistry images are shown at the intermediate dose of 6×10^{12} vg total. Immunofluorescent staining for micro-dystrophin using an N-terminal dystrophin antibody in the TA, heart, and DIA 3 months postinjection compared to Lactated Ringer's (vehicle)-treated *mdx* mice (second *row* panel). β-sarcoglycan staining in the treated cohorts represent rescue of the dystrophin-associated protein complex. **(B)** Quantification of immunofluorescent-positive fibers expressing dystrophin protein. Data are reported as mean $\pm$ SEM of $n=5$ per treatment group. DIA, diaphragm; GAS, gastrocnemius; GLUT, gluteus; *mdx*-LR, Lactated Ringer's (vehicle)-treated *mdx*; PSO, psoas major; QD, quadriceps; SEM, standard error of the mean; TA, tibialis anterior; TRI, triceps.

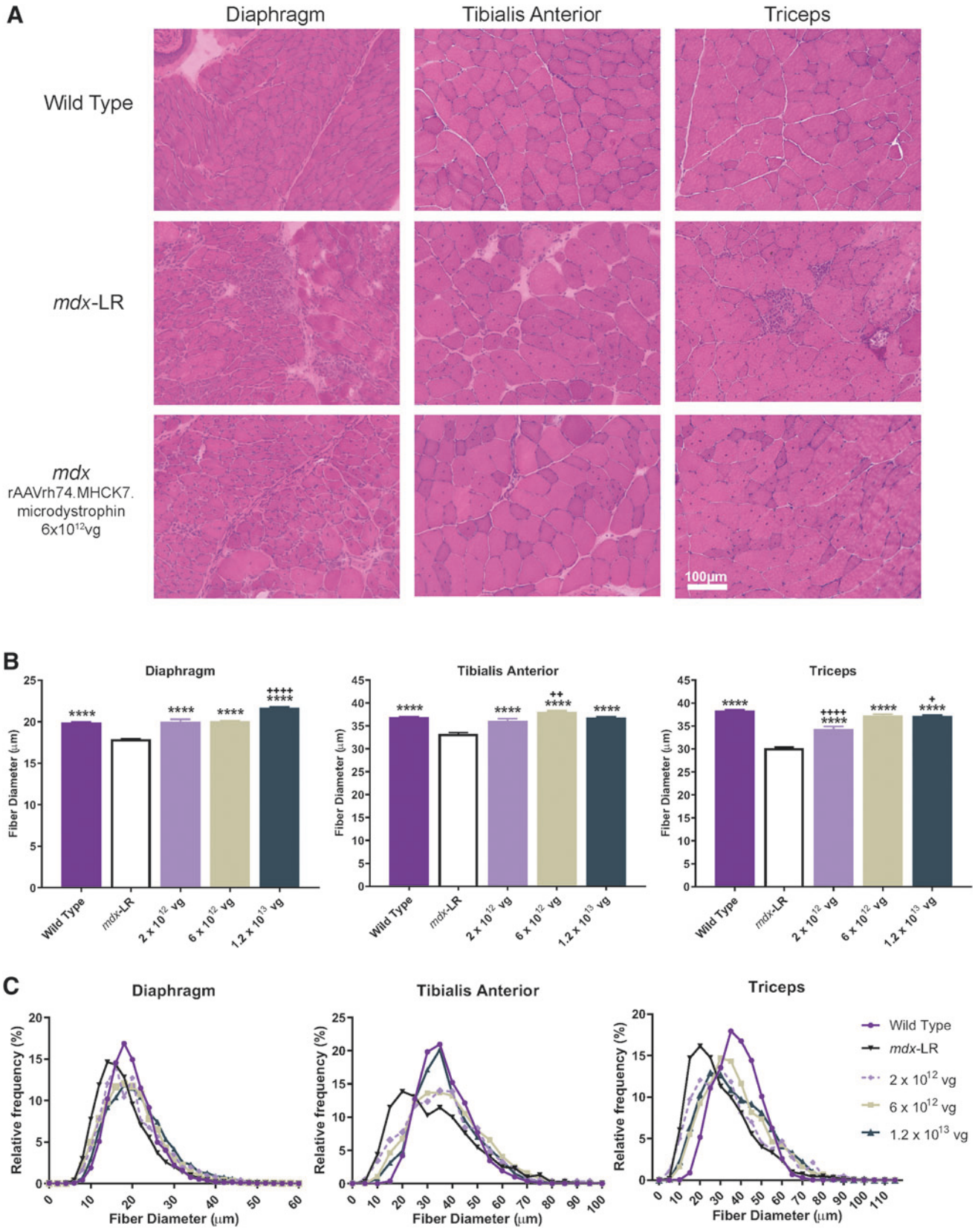

Figure 2. Systemic treatment with rAAVrh74.MHCK7.micro-dystrophin improves muscle pathology in *mdx* mice. Hematoxylin and eosin staining to detect morphology. **(A)** Representative images of diaphragm, tibialis anterior, and triceps muscle from WT mice, Lactated Ringer's (vehicle)-treated *mdx* mice (*mdx*-LR mice), and rAAVrh74.MHCK7.micro-dystrophin-treated *mdx* mice at the intermediate dose of 6×10^{12} vg total. **(B, C)** Quantification of average fiber size and frequency distribution demonstrates a normalization of fiber size across all of the assessed tissues (*i.e.*, diaphragm, tibialis anterior, and triceps) in the *mdx* mice treated with rAAVrh74.MHCK7.micro-dystrophin at total dose of 2×10^{12} vg, 6×10^{12} vg, and 1.2×10^{13} vg. Data reported in bar graph as mean ± SEM ($n=4$ low dose ($SD_{DIA}=7.4$, $SD_{TA}=15.1$, $SD_{TRI}=17.3$); $n=8$ intermediate dose ($SD_{DIA}=7.2$, $SD_{TA}=14.1$, $SD_{TRI}=15.2$) and high dose ($SD_{DIA}=7.9$, $SD_{TA}=12$, $SD_{TRI}=15.8$); $n=6$ *mdx*-LR ($SD_{DIA}=6.6$, $SD_{TA}=15.8$, $SD_{TRI}=15.1$); and WT ($SD_{DIA}=5.6$, $SD_{TA}=10$, $SD_{TRI}=10.6$)). Data were analyzed by one-way ANOVA followed by Tukey's *post hoc* analysis. **** = $p<0.0001$ versus *mdx*-LR mice. + = $p<0.5$; ++ = $p<0.005$; ++++ = $p<0.0001$ versus WT. ANOVA, analysis of variance; SD, standard deviation; WT, wild-type.

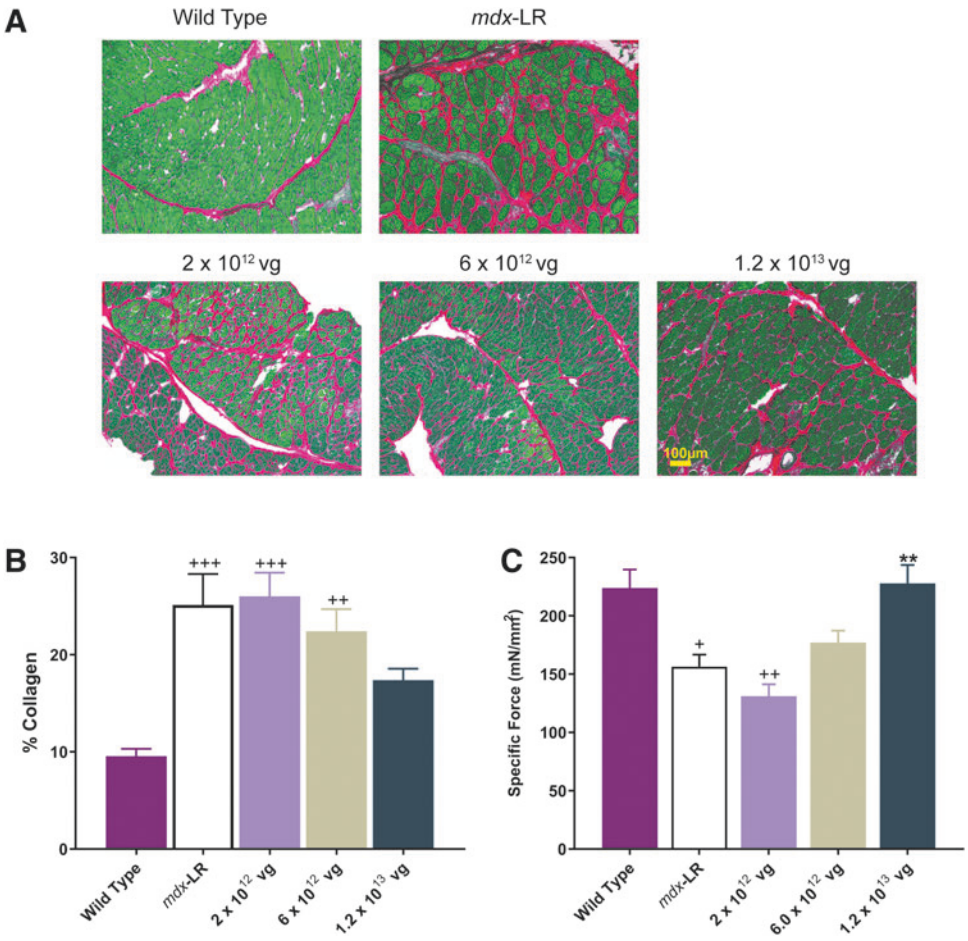

Figure 3. Reduction of fibrosis after systemic treatment with rAAVrh74.MHCK7.micro-dystrophin is associated with improvement in DIA muscle function. Muscle tissue sections were stained using picrosirius red stain to assess collagen content. **(A)** Representative images of DIA tissue sections in WT mice, Lactated Ringer's (vehicle)-treated *mdx* mice (*mdx*-LR mice), and *mdx* mice treated with rAAVrh74.MHCK7.micro-dystrophin with low (2×10^{12} vg), intermediate (6×10^{12} vg), and high (1.2×10^{13} vg) doses. **(B)** Quantification of collagen accumulation (%) in the DIA of WT mice, *mdx*-LR mice, and *mdx* mice treated with rAAVrh74.MHCK7.micro-dystrophin ($n=5$, low dose; $n=8$, intermediate and high dose; $n=6$, *mdx*-LR; and $n=5$, WT). **(C)** DIA muscle function in WT mice, *mdx*-LR mice, and *mdx* mice treated with rAAVrh74.MHCK7.micro-dystrophin ($n=5$, low dose; $n=9$, intermediate; $n=8$, high dose; $n=8$, *mdx*-LR; and $n=5$, WT). Following 3 months of treatment, DIA muscle strips were harvested to measure specific force (normalized to cross-sectional area). For panels **B** and **C**, data are represented as mean ± SEM and were analyzed by one-way ANOVA followed by Tukey's *post hoc* analysis. ** = $p<0.005$ versus *mdx*-LR mice; + = $p<0.05$, ++ = $p<0.005$, +++ = $p<0.001$ versus WT mice.

increasing improvement compared to the untreated mice with no significant differences between the highest dose and the WT (Fig. 3B), which corresponded to a significant increase in force output of the DIA to levels comparable to that observed in WT mice (Fig. 3C). Finally, to evaluate the presence of any additional histopathology in the skeletal muscles due to vector delivery, an alpha sarcomeric actin immunofluorescent stain was used to evaluate any incidence of ringed fibers. Previously, others have described incidences of ringed fibers in the neuromuscular junction or the GAS with the inclusion of a micro-dystrophin construct that contains the H2 region.[35,47,48] After a thorough analysis of all skeletal muscles, there were no instances of ringed fibers or abnormal histopathology in *mdx* mice after treatment with rAAVrh74.MHCK7.micro-dystrophin (Supplementary Fig. S3).

Functional improvements with systemic delivery in dose-dependent manner

To determine whether micro-dystrophin gene transfer provides a functional benefit to diseased muscle, we assessed the properties of both the DIA (Fig. 3C) and TA (Fig. 4A, B) muscles from WT mice, *mdx*-LR mice, and rAAVrh74.MHCK7.micro-dystrophin-treated mice at the three dose levels. Tail vein delivery of rAAVrh74.MHCK7.micro-dystrophin led to a stepwise improvement in specific force output in the DIA (176.9 mN/mm^2 in the intermediate-dose group vs. 227.78 mN/mm^2 in the high-dose group) that was comparable to WT levels for the higher dose. Furthermore, it was demonstrated that, for the TA muscle, there were functional deficits in *mdx*-LR mice compared with WT mice with a 58% decrease in force output (171.3 vs. 291.65 mN/mm^2)

and greater loss of force following eccentric contractions (32% loss in *mdx*-LR mice; 5% loss in WT mice). Administration of rAAVrh74.MHCK7.micro-dystrophin resulted in a significant improvement in force output and rescue from contraction-induced damage in the TA muscles after rigorous eccentric contraction exercise. Finally, the systemic delivery of the rAAVrh74.MHCK7.micro-dystrophin construct, which contains the critical force producing spectrin repeats R1–R3, demonstrates increased force generation in the TA and DIA. Furthermore, micro-dystrophin significantly protected muscle membranes from damage, as evidenced by a 75% reduction of creatine kinase (CK) (Fig. 4C).

In addition to sarcoglycan proteins, we also evaluated other DAPC-associated components, such as nNOS, using western blot analysis. Although the micro-dystrophin construct does not contain spectrin repeats 16 and 17, which have been identified as one of the sarcolemmal nNOS-specific sites,[49,50] when analyzing nNOS protein expression by western blot for all muscles analyzed in treated animals ($n=2$ analyzed), we found the amount of nNOS protein in skeletal muscle to be equal to the amount found in WT TA tissues and increased compared to the untreated *mdx* mouse (Fig. 5A).

Vector biodistribution following systemic delivery

To confirm the presence of test article-specific DNA sequences, biodistribution analysis was examined using real-time qPCR. Figure 5B depicts the vg copies detected in each tissue sample from rAAVrh74.MHCK7.micro-dystrophin-injected mice. rAAVrh74.MHCK7.micro-dystrophin transcript was detected at varying levels in all collected tissues. As expected, the highest levels were seen in skeletal muscle and the heart, as well as clearance organs. The lowest levels were detected in gonad, lung, and kidney in all dose levels. Western blot was used to detect the transgene micro-dystrophin protein in tissue samples. Micro-dystrophin protein was observed across all skeletal muscles analyzed, with the highest amount in the heart for intermediate and high dose (representative Fig. 5C, full blot in Supplementary Fig. S5, additional animal blots in Supplementary Fig. S6). Importantly there was no micro-dystrophin protein detected in the intermediate and high dose cohorts in any off-target organs. We observed a faint band in the liver at the highest dose, which could be at the lower limit of detection. Finally, there were no adverse histopathologic effects noted in the liver by the independent pathologist and no abnormal blood chemistries in any of the dosed cohorts (Supplementary Fig. S4).

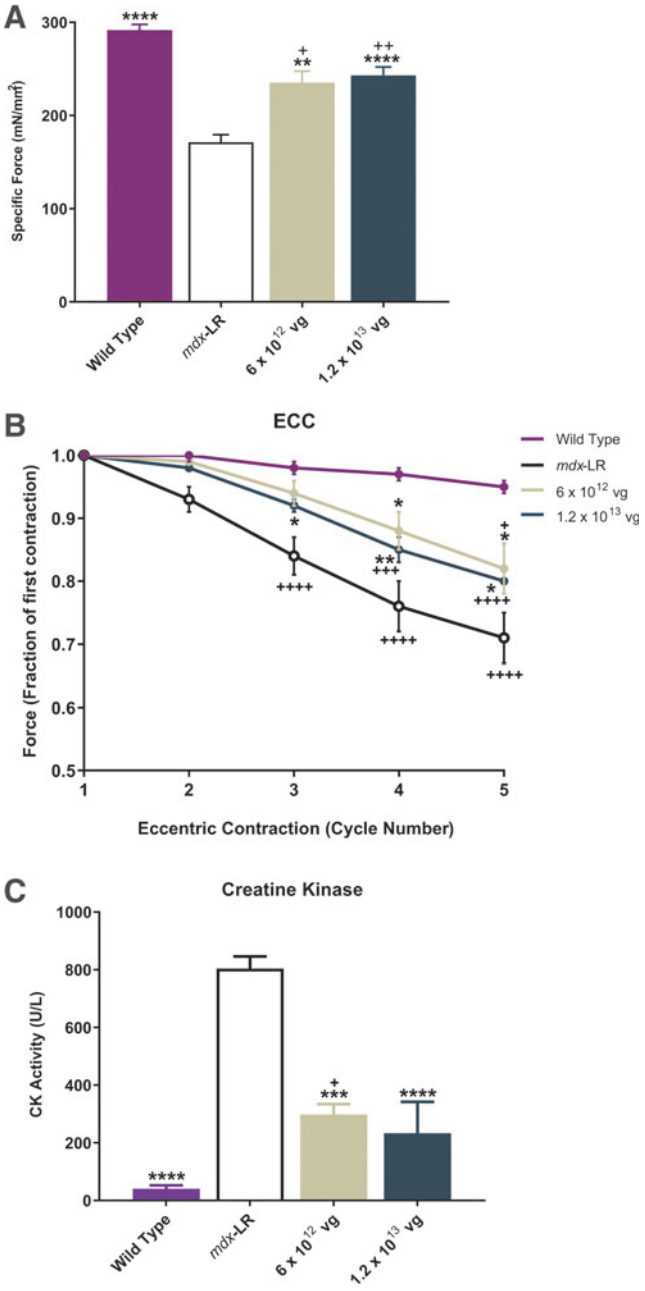

Figure 4. Functional benefits to skeletal muscle in intermediate- and high-dose cohorts. **(A)** Specific muscle force in TA muscles (normalized to cross-sectional area) assessed 3 months after treatment with rAAVrh74.MHCK7.micro-dystrophin (*left* and *right* side per animal, per cohort: $n=8$, intermediate dose (6×10^{12} vg); $n=16$, high dose (1.2×10^{13} vg); $n=14$, Lactated Ringer's (vehicle)-treated *mdx* (*mdx*-LR); $n=9$, WT). **(B)** Eccentric force loss in TA muscle assessed using a rigorous ECC protocol. Force output is plotted at each cycle (mean of *left* and *right* side per animal, per cohort: $n=8$, intermediate dose; $n=13$, high dose; $n=13$, *mdx*-LR; $n=9$, WT). **(C)** Serum CK levels 3 months post-treatment ($n=2$, intermediate and high dose; $n=5$, *mdx*-LR and WT). For panels **A** and **C**, data are represented as mean ± SEM and analyzed by one-way ANOVA followed by Tukey's *post hoc* analysis for multiple comparisons. $**=p<0.01$, $***=p<0.001$, and $****=p<0.0001$ versus *mdx*-LR mice; $+=p<0.05$, $++=p<0.005$, $+++=p<0.001$, $++++=p=0.0001$ versus WT mice. In panel **B**, data are represented as mean ± SEM and analyzed by two-way ANOVA followed by Tukey's *post hoc* analysis for multiple comparisons. $*=p<0.05$, $**=p<0.01$ versus *mdx*-LR mice; $+=p<0.05$, $+++=p<0.001$, $++++=p=0.0001$ versus WT mice. CK, creatine kinase; ECC, eccentric contraction cycle.

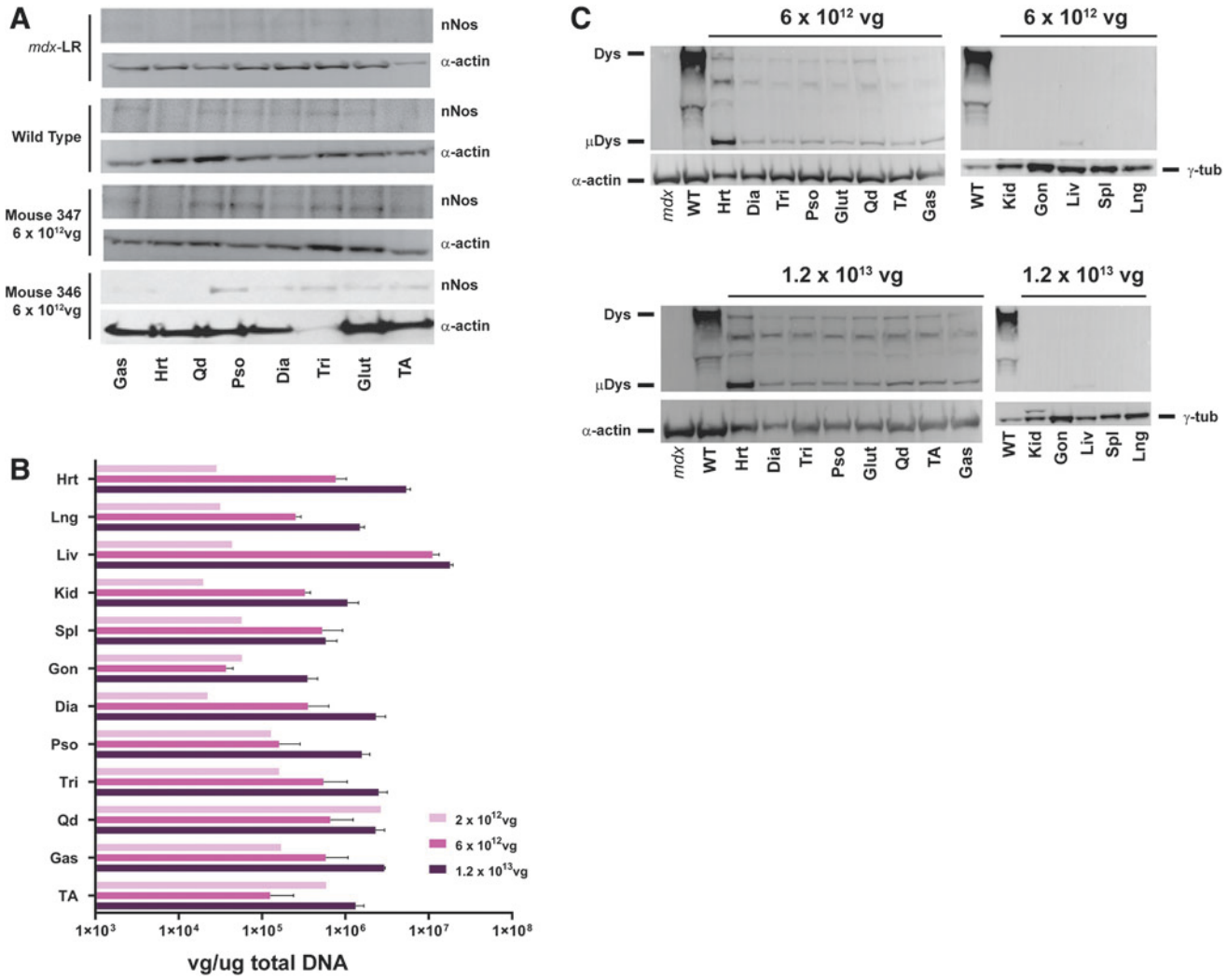

Figure 5. Biodistribution of vgs and protein expression in vector-treated mice. **(A)** Representative western blot of nNOS protein expression in muscle tissues of Lactated Ringer's (vehicle)-treated *mdx* mice, WT mice, and two mice (Mouse 347 and Mouse 346) treated with 6×10^{12} vg total dose of rAAVrh74.MHCK7.micro-dystrophin (intermediate). **(B)** Biodistribution of vgs normalized to microgram of DNA in organs and tissues after systemic delivery of rAAVrh74.MHCK7.micro-dystrophin ($n=3$ for each cohort). Data are represented as mean ± SEM. **(C)** Western blot analysis of dystrophin protein expression in muscles and organs from mice 3 months after treatment with rAAVrh74.MHCK7.micro-dystrophin at an intermediate (6×10^{12} vg) and high (1.2×10^{13} vg) dose. α-actinin and γ-tubulin were used as loading controls. α-actin, α-actinin; Dys, dystrophin; γ-tub, γ-tubulin; Glut, gluteus; Gon, gonads; Hrt, heart; Kid, kidney; Liv, liver; Lng, lung; μDys, micro-dystrophin; *mdx*-LR, Lactated Ringer's (vehicle)-treated *mdx*; nNOS, neuronal nitric oxide synthase; Spl, spleen.

Durable improvements following a single systemic infusion

A cohort of *mdx* male mice were injected with an intermediate dose (6×10^{12} vg) at 4 weeks of age and necropsied at 6 months postinjection to evaluate long-term expression and functional benefit of a single intravenous treatment with rAAVrh74.MHCK7.micro-dystrophin. Micro-dystrophin transgene expression was demonstrated using immunofluorescent staining for micro-dystrophin using an N-terminal dystrophin antibody in skeletal muscle (TA), heart, and DIA (Fig. 6A). Histology was analyzed by hematoxylin and eosin staining (Fig. 6B). Micro-dystrophin transgene expression was also evaluated by immunofluorescence in six skeletal muscles (TA, GAS, QD, PSO, TRI, GLUT), both left and right, in addition to the DIA of all treated mice. Systemic delivery of an intermediate dose (6×10^{12} vg) of rAAVrh74.MHCK7.micro-dystrophin resulted in 65.5% fibers localized to the membrane with micro-dystrophin in the TA muscle (Fig. 6C) and an increase of specific force output, which improved to 235.4 mN/mm^2 and protected the muscle from repeated eccentric contraction damage with only a 25% decrease in force (Fig. 6D). These results demonstrate that there was preservation of transgene expression 6 months postinjection, as well as no decrease in functional benefits observed at earlier time points in both the DIA and TA, suggesting sustained effects (long-term durability) after a single administration.

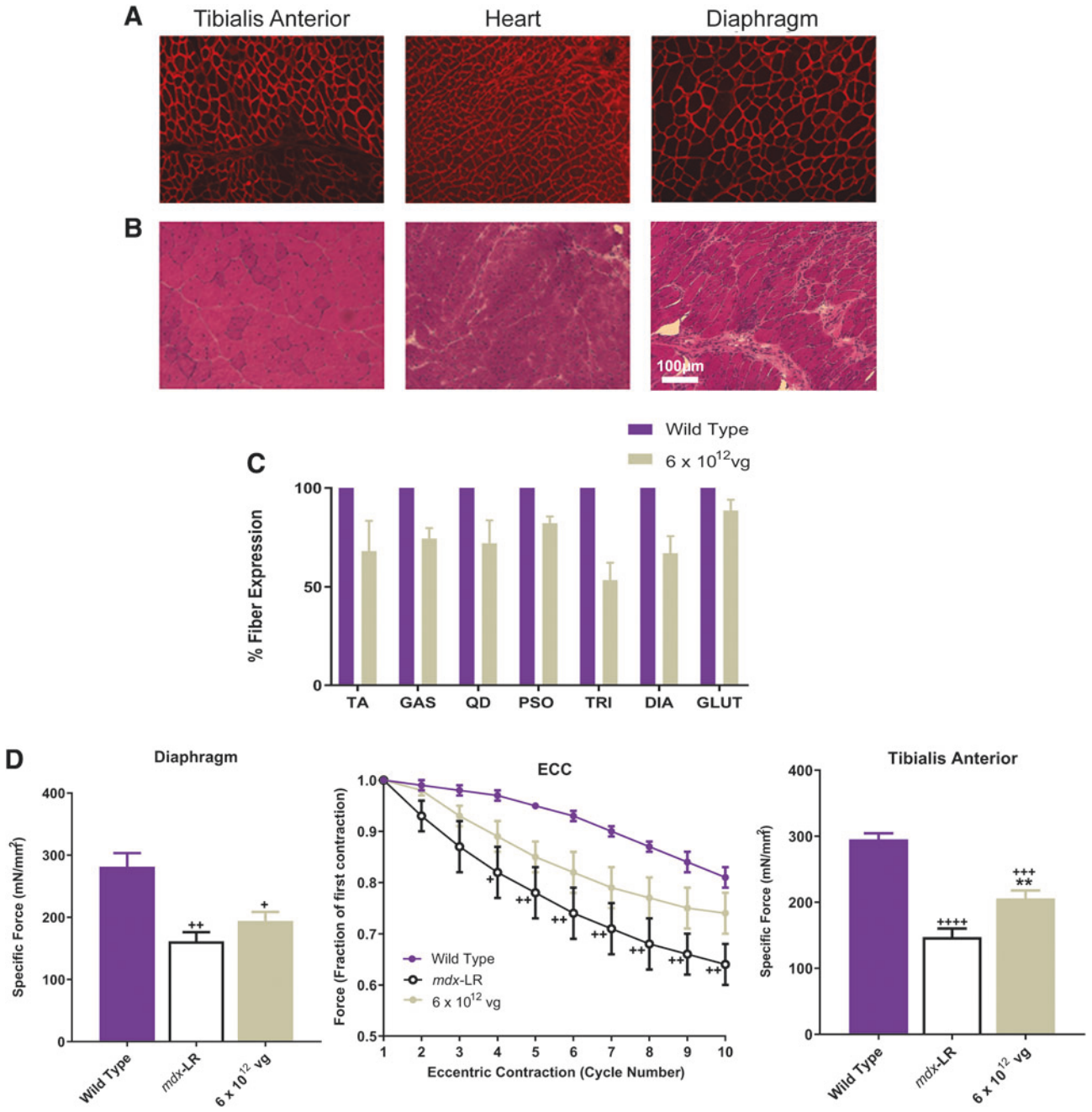

Figure 6. Long-term durability after a single administration of rAAVrh74.MHCK7.micro-dystrophin in *mdx* mice. **(A, B)** Representative immunofluorescent staining for micro-dystrophin using an N-terminal dystrophin antibody and hematoxylin and eosin stained TA, heart, and DIA of *mdx* mice treated with rAAVrh74.micro-dystrophin at an intermediate (6×10^{12} vg) dose, 6 months post-treatment. **(C)** Quantification of immunofluorescent-positive fibers expressing micro-dystrophin protein 6 months after a single treatment with rAAVrh74.MHCK7.micro-dystrophin. Data are reported as mean ± SEM of $n=5$. **(D)** Specific force generation in the DIA and TA muscles 6 months after a single treatment with rAAVrh74.MHCK7.micro-dystrophin. Data reported as mean ± SEM of $n=5$. Data were analyzed by one-way ANOVA followed by Tukey's *post hoc* analysis for multiple comparisons. **$=p<0.05$ versus *mdx*-LR mice; +$=p<0.05$, ++$=p<0.005$, +++$=p<0.0005$, ++++$=p<0.0001$ versus WT mice. Eccentric force loss following a rigorous ECC protocol ($n=8$ in each group). Data reported as mean ± SEM. Data were analyzed by two-way ANOVA followed by Tukey's *post hoc* analysis for multiple comparisons. +$=p<0.2$, ++$=p<0.007$ versus WT mice. Glut, gluteus; *mdx*-LR, Lactated Ringer's (vehicle)-treated *mdx*.

DISCUSSION

We have designed a therapeutic human micro-dystrophin cassette packaged into an rAAVrh74 vector, which includes the use of a dual striated muscle-specific promoter to selectively express transgene in skeletal and cardiac muscle. rAAVrh74 is a serotype recently isolated from lymph nodes of rhesus monkeys. rAAVrh74 displays high affinity for skeletal and cardiac muscle tissue,[51,52] and we have previously demonstrated robust biopotency using rAAVrh74 in biodistribution, delivery, and trans-

duction of dysferlin, GALGT, and sarcoglycan proteins for other muscular dystrophies.[36,51–54] In addition, rAAVrh74 seroprevalence is relatively low among other AAV serotypes,[55] which thus allows for application for more patients. Currently, the rAAVrh74 capsid is the vector that we have used in our gene therapy clinical trials in patients with DMD and with limb-girdle muscular dystrophy types 2E/R4, 2D/R3, and 2B/R2 (NCT02376816, NCT03769116, NCT03652259, NCT01976091, NCT02710500).

The safety and efficacy of AAV gene therapy for neuromuscular diseases are not only dictated by vector delivery (*e.g.*, biodistribution and tissue uptake) but also by regulation of transgene expression in the targeted tissue (*i.e.*, skeletal and cardiac muscle). Use of selective promoters is essential to maximize gene expression in targeted tissues and limit expression in nonrelevant tissues. In this study, we used MHCK7, which includes an α-MHC enhancer that has been shown to lead to high levels of expression in cardiomyocytes and increased dystrophin expression in skeletal muscle compared to muscle-specific promoters, MCK or CK7.[32] Indeed, we provide further support that MHCK7 limits off-target transgene expression, as demonstrated by widespread tissue and organ biodistribution of vector genomes, accompanied by micro-dystrophin protein expression limited to skeletal and cardiac muscle. Our findings presented here are consistent with our previous studies that demonstrated robust skeletal and cardiac muscle expression of *β*-sarcoglycan in mice after systemic delivery of the transgene using the rAAVrh74 capsid with expression driven by MHCK7.[39]

In the present study we provide further evidence that demonstrates the translational relevance of systemic delivery of rAAVrh74.MHCK7.micro-dystrophin. Systemic delivery of rAAVrh74.MHCK7.micro-dystrophin demonstrated prevention of dystrophic features at both the intermediate and high doses with reductions in inflammation, fewer degenerating fibers, and improvement in force generation of the DIA and the TA. The reductions in dystrophic histopathology were more marked in the intermediate- and high-dose cohorts, with no significant difference in decreased degeneration and decreased inflammation between the two dosing groups. The DIA revealed the most marked changes in dosed cohorts. The heart exhibited a few small foci of minimal mononuclear cell accumulation in the ventricular myocardium in several dosed animals. However, vector-dosed cohorts had substantially reduced myopathy in all tissues and the heart. Of interest, serum CK levels were significantly reduced after treatment with rAAVrh74.MHCK7.micro-dystrophin, which coincides with the protection we observed from damage due to eccentric contractions in vector-dosed *mdx* mice compared to *mdx*-LR mice.

It must be noted that given the limited DNA packaging capacity of AAV, numerous efforts to develop and evaluate shortened variations of dystrophin have been examined in preclinical animal models. While many constructs have shown success in delivery, varying degrees of expression and functional efficacy have been reported (for review, see Duan[56]). We chose to use a transgene sequence designed to result in production of a protein with optimized functionality. Indeed, the transgene utilized here (ΔR4-23/ΔCT) has been shown to prevent and reverse dystrophic pathology associated in *mdx* mice and protect against damage due to eccentric contractions when delivered using AAV2, AAV6, or AAV8 with expression driven by the cytomegalovirus (CMV) or the muscle-specific promoter, MCK.[34,57,58] This variant of micro-dystrophin includes the N-terminus; spectrin-like repeats R1-3 and R24; hinges 1, 2, and 4; and the cysteine-rich domain. We believe that the ability of R1-3 to interact with the lipid membrane[29,30] may play an important role in maintaining structural integrity and protection of muscle tissue from damage.

In addition, inclusion of hinges is important for conferring flexibility by providing the structural mechanism for dystrophin to function as a shock absorber.[24] Prior studies reported that the presence of hinge 3 in ΔR4-23/ΔCT rescued muscle deterioration and structural deficits at neuromuscular junctions in *mdx* mice.[58] However, there were no differences in restoration of muscle functional capacity between hinge 2 and hinge 3 when configured in micro-dystrophin constructs ΔR4-23/ΔCT and ΔH2-23/ΔCT+H3 in *mdx* mice.[58] Banks *et al.* reported the formation of ringed fibers in *mdx* mice expressing ΔR4-23/ΔCT packaged into AAV6 with expression of the transgene driven by the constitutive CMV promoter.[58] In the present study, we did not observe any instance of ringed fibers in any vector-dosed tissues in mice. The reason for this discrepancy is unclear but could be due to differences in the constructs or technical differences between studies (*e.g.*, age of mice, route of administration). Use of hinge 2 has the advantage of maintaining the natural linkage to the R1–3 domain, whereas use of hinge 3 would create a novel junction. Novel juxtapositions of protein domains may promote immune responses[59] or result in protein misfolding, which in turn may either promote degradation[60,61] or result in formation of protein inclusions.[34,62]

It has been reported that nNOS binding domain R16–17 of dystrophin is essential to restore sarcolemmal nNOS expression in *mdx* mice and canine DMD models, as demonstrated by enhanced muscle perfusion, prevention of functional ischemia, and improvement in muscle force and exercise capacity.[19,28,48,63–65] In contrast, several lines of evidence have also demonstrated that while lack of nNOS expression may be sufficient to promote deterioration, its presence is not required for muscle function or protection from overt dystrophy. For example, mice with genetic loss of nNOSμ did not exhibit skeletal muscle fatigue or loss of specific muscle force,[66] and forced expression of nNOSμ only partially rescued eccentric force loss in mouse models of DMD compared to WT animals.[67] Likewise, the presence of the R16–17 domains in micro-dystrophin

constructs only partially protected the eccentric force loss observed in *mdx* mice.[28] Furthermore, transgenic mouse models that harbor genetic loss of nNOS expression do not overtly display a dystrophic phenotype.[68,69]

In the present study, we analyzed nNOS expression for two treated mice from the intermediate-dose cohort, and the results show increased quantities of nNOS protein in all skeletal muscles compared with *mdx*-LR mice. These results are preliminary and further studies are needed, but suggest that nNOS protein presence in the muscle rather than increased nNOS sarcolemma-specific localization is beneficial for function, as has been previously suggested.[16,17]

Altogether these studies, in conjunction with the present findings, demonstrate the importance in design and configuration of micro-dystrophin.

In addition to efficacy, this dose-escalation study demonstrated minimal toxicity when mice were treated with rAAVrh74.MHCK7.micro-dystrophin at even the highest total dose of 1.2×10^{13} vg. In *mdx*-LR mice there was widespread variable myopathy affecting all seven skeletal muscles, as well as the right ventricular wall of the heart. The principal findings included pronounced and widespread myofiber atrophy (30–75% of normal myofiber size), minimal-to-mild mononuclear cell inflammations, increased interstitial space, and increased cytoplasmic mineral deposits, as concluded by an independent veterinary pathologist. Notably, the lack of abnormal values in evaluation using a serum chemistry panel further provides support for the safety and tolerability to treatment with rAAVrh74.MHCK7.micro-dystrophin.

In conclusion, the findings presented here provide proof of principle for safety and efficacy to support systemic delivery of rAAVrh74.MHCK7.micro-dystrophin at high vector titers and support initiation of a Phase I/II safety study in patients with DMD.

ACKNOWLEDGMENTS

The authors thank the Nationwide Children's Viral Vector Core for Vector Production and Dr. Stephen Hauschka for his gift of the MHCK7 promoter. The authors also thank Terri Shaffer, MLAS, RLATG, for performing intravenous tail vein injections. Medical writing and editorial support were provided by Khampaseuth Thapa, PhD, and Lucia Quintana-Gallardo, PhD, of Sarepta Therapeutics, Inc., and Purvi Kobawala Smith, MS, MPH, of Health & Wellness Partners, LLC, Upper Saddle River, NJ, funded by Sarepta Therapeutics, Inc.

AUTHORS' CONTRIBUTIONS

Conceptualization, R.A.P., J.R.M., and L.R.R.-K.; Methodology, R.A.P., D.A.G., and L.R.R.-K.; Formal analysis, R.A.P; Investigation, R.A.P, D.A.G., K.N.H, E.L.P., and E.K.C.; Resources, R.A.P, D.A.G, L.R.R.-K.; Writing—original draft, R.A.P., and L.R.R.-K.; Writing—review & editing, R.A.P., D.A.G, K.N.H, J.R.M., and L.R.R.-K.; Visualization, R.A.P, D.A.G., J.R.M, and L.R.R.-K.; Supervision, L.R.R.-K.; Project administration, D.A.G.; Funding acquisition, J.R.M. and L.R.R.-K.

AUTHOR DISCLOSURE

R.A.P. is an employee of Sarepta Therapeutics, Inc., D.A.G. is an employee of Sarepta Therapeutics, Inc., K.N.H. and E.K.C.: No competing financial interest exists. E.L.P. is an employee of Sarepta Therapeutics, Inc., J.R.M. is the coinventor of the rAAVrh74.micro-dystrophin technology. This technology has been exclusively licensed to Sarepta Therapeutics, Inc., L.R.R.-K. is the coinventor of the AAVrh74.micro-dystrophin technology and eligible to receive financial consideration as a result. L.R.R.-K. is an employee of Sarepta Therapeutics, Inc.

FUNDING INFORMATION

This study was funded by the Nationwide Children's Hospital Research Foundation, Parent Project Muscular Dystrophy, and Sarepta Therapeutics, Inc.

SUPPLEMENTARY MATERIAL

Supplementary Figure S1
Supplementary Figure S2
Supplementary Figure S3
Supplementary Figure S4
Supplementary Figure S5
Supplementary Figure S6
Supplementary Table S1

REFERENCES

1. Aartsma-Rus A, Straub V, Hemmings R, et al. Development of exon skipping therapies for Duchenne muscular dystrophy: a critical review and a perspective on the outstanding issues. Nucleic Acid Ther 2017;27:251–259.
2. Emery AE. Population frequencies of inherited neuromuscular disease—a world survey. Neuromuscul Disord 1991;1:19–29.
3. Mendell JR, Lloyd-Puryear M. Report of MDA muscle disease symposium on newborn screening for Duchenne muscular dystrophy. Muscle Nerve 2013;48:21–26.
4. Mendell JR, Shilling C, Leslie ND, et al. Evidence based path to newborn screening for Duchenne muscular dystrophy. Ann Neurol 2012;71:304–313.
5. Oudet C, Hanauer A, Clemens P, et al. Two hot spots of recombination in the DMD gene correlate with the deletion prone regions. Hum Mol Genet 1992;1:599–603.
6. Brooke MH, Fenichel GM, Griggs RC, et al. Clinical investigation in Duchenne dystrophy: 2. Determination of the "power" of therapeutic trials based on the natural history. Muscle Nerve 1983;6:91–103.

7. Birnkrant DJ, Bushby K, Bann CM, et al. Diagnosis and management of Duchenne muscular dystrophy, part 1: diagnosis, and neuromuscular, rehabilitation, endocrine, and gastrointestinal and nutritional management. Lancet Neurol 2018;17: 251–267.

8. Liu D, Ahmet A, Ward L, et al. A practical guide to the monitoring and management of the complications of systemic corticosteroid therapy. Allergy Asthma Clin Immunol 2013;9:30.

9. Cirak S, Arechavala-Gomeza V, Guglier M, et al. Exon skipping and dystrophin restoration in patients with Duchenne muscular dystrophy after systemic phosphorodiamidate morpholino oligomer treatment: an open-label, phase 2, dose-escalation study. Lancet 2011;378:595–605.

10. Exondys 51 (eteplirsen) [prescribing information]. Cambridge, MA: Sarepta Therapeutics, Inc., 2018.

11. Mendell JR, Goemans N, Lowes LP, et al. Longitudinal effect of eteplirsen versus historical control on ambulation in Duchenne muscular dystrophy. Ann Neurol 2016;79:257–271.

12. Khan N, Eliopoulos H, Han L, et al. Eteplirsen treatment attenuates respiratory decline in ambulatory and non-ambulatory patients with Duchenne muscular dystrophy. J Neuromuscul Dis 2019;6:213–225.

13. Frank DE, Schnell FJ, Akana C, et al. Increased dystrophin production with golodirsen in patients with Duchenne muscular dystrophy. Neurology 2020;94:e2270–e2282.

14. Clemens PR, Rao VK, Connolly AM, et al. Safety, tolerability, and efficacy of viltolarsen in boys with Duchenne muscular dystrophy amenable to exon 53 skipping: a phase 2 randomized clinical trial. JAMA Neurol 2020;77:982–991.

15. Gregorevic P, Blankinship MJ, Allen JM, et al. Systemic microdystrophin gene delivery improves skeletal muscle structure and function in old dystrophic *mdx* mice. Mol Ther 2008;16:657–664.

16. Koo T, Okada T, Athanasopoulos T, et al. Long-term functional adeno-associated virus-microdystrophin expression in the dystrophic CXMDj dog. J Gene Med 2011;13:497–506.

17. Le Guiner C, Servais L, Montus M, et al. Long-term microdystrophin gene therapy is effective in a canine model of Duchenne muscular dystrophy. Nat Commun 2017;8:16105.

18. Liu M, Yue Y, Harper SQ, et al. Adeno-associated virus-mediated microdystrophin expression protects young *mdx* muscle from contraction-induced injury. Mol Ther 2005;11:245–256.

19. Shin JH, Pan X, Hakim CH, et al. Microdystrophin ameliorates muscular dystrophy in the canine model of duchenne muscular dystrophy. Mol Ther 2013;21:750–757.

20. Yue Y, Li Z, Harper SQ, et al. Microdystrophin gene therapy of cardiomyopathy restores dystrophin-glycoprotein complex and improves sarcolemma integrity in the *mdx* mouse heart. Circulation 2003;108:1626–1632.

21. Dongsheng D. Micro-dystrophin gene therapy goes systemic in Duchenne muscular dystrophy patients. Hum Gene Ther 2018;29:733–736.

22. Norwood FL, Sutherland-Smith AJ, Keep NH, et al. The structure of the N-terminal actin-binding domain of human dystrophin and how mutations in this domain may cause Duchenne or Becker muscular dystrophy. Structure 2000;8: 481–491.

23. Crawford GE, Faulkner JA, Crosbie RH, et al. Assembly of the dystrophin-associated protein complex does not require the dystrophin COOH-terminal domain. J Cell Biol 2000;150:1399–1410.

24. Koenig M, Kunkel LM. Detailed analysis of the repeat domain of dystrophin reveals four potential hinge segments that may confer flexibility. J Biol Chem 1990;265:4560–4566.

25. Suzuki A, Yoshida M, Yamamoto H, et al. Glycoprotein-binding site of dystrophin is confined to the cysteine-rich domain and the first half of the carboxy-terminal domain. FEBS Lett 1992;308: 154–160.

26. Jung D, Yang B, Meyer J, et al. Identification and characterization of the dystrophin anchoring site on beta-dystroglycan. J Biol Chem 1995;270: 27305–27310.

27. Harper SQ, Crawford RW, DelloRusso C, et al. Spectrin-like repeats from dystrophin and alpha-actinin-2 are not functionally interchangeable. Hum Mol Genet 2002;11:1807–1815.

28. Nelson DM, Lindsay A, Judge LM, et al. Variable rescue of microtubule and physiological phenotypes in *mdx* muscle expressing different miniaturized dystrophins. Hum Mol Genet 2018;27: 2090–2100.

29. Legardinier S, Hubert JF, Le Bihan O, et al. Subdomains of the dystrophin rod domain display contrasting lipid-binding and stability properties. Biochim Biophys Acta 2008;1784:672–682.

30. Zhao J, Kodippili K, Yue Y, et al. Dystrophin contains multiple independent membrane-binding domains. Hum Mol Genet 2016;25:3647–3653.

31. Rodino-Klapac LR, Janssen PM, Montgomery CL, et al. A translational approach for limb vascular delivery of the micro-dystrophin gene without high volume or high pressure for treatment of Duchenne muscular dystrophy. J Transl Med 2007;5: 45.

32. Salva MZ, Himeda CL, Tai PW, et al. Design of tissue-specific regulatory cassettes for high-level rAAV-mediated expression in skeletal and cardiac muscle. Mol Ther 2007;15:320–329.

33. Rodino-Klapac LR, Janssen PM, Shontz KM, et al. Micro-dystrophin and follistatin co-delivery restores muscle function in aged DMD model. Hum Mol Genet 2013;22:4929–4937.

34. Rodino-Klapac LR, Montgomery CL, Bremer WG, et al. Persistent expression of FLAG-tagged micro dystrophin in nonhuman primates following intramuscular and vascular delivery. Mol Ther 2010; 18:109–117.

35. Harper SQ, Hauser MA, DelloRusso C, et al. Modular flexibility of dystrophin: implications for gene therapy of Duchenne muscular dystrophy. Nat Med 2002;8:253–261.

36. Sondergaard P, Griffin D, Pozsgai E, et al. AAV .dysferlin overlap vectors restore function in dysferlinopathy animal models. Ann Clin Transl Neurol 2015;2:256–270.

37. Mendell JR, Rodino-Klapac LR, Rosales XQ, et al. Sustained alpha-sarcoglycan gene expression after gene transfer in limb-girdle muscular dystrophy, type 2D. Ann Neurol 2010;68:629–638.

38. Schnepp BC, Jensen RL, Chen CL, et al. Characterization of adeno-associated virus genomes isolated from human tissues. J Virol 2005;79: 14793–14803.

39. Pozsgai ER, Griffin DA, Heller KN, et al. Systemic AAV-mediated β-sarcoglycan delivery targeting cardiac and skeletal muscle ameliorates histological and functional deficits in LGMD2E mice. Mol Ther 2017;25:855–869.

40. Beastrom N, Lu H, Macke A, et al. *mdx*^{5cv} mice manifest more severe muscle dysfunction and diaphragm force deficits than do *mdx* Mice. Am J Pathol 2011;179:2464–2474.

41. Rafael-Fortney JA, Chimanji NS, Schill KE, et al. Early treatment with lisinopril and spironolactone preserves cardiac and skeletal muscle in Duchenne muscular dystrophy mice. Circulation 2011;124:582–588.

42. Moorwood C, Liu M, Tian Z, et al. Isometric and eccentric force generation assessment of skeletal muscles isolated from murine models of muscular dystrophies. J Vis Exp 2013;71:e50036.

43. Heller KN, Montgomery CL, Shontz KM, et al. Human α7 integrin gene (*ITGA7*) delivered by adeno-associated virus extends survival of severely affected dystrophin/utrophin-deficient mice. Hum Gene Ther 2015;26:647–656.

44. Hakim CH, Li D, Duan D. Monitoring murine skeletal muscle function for muscle gene therapy. Methods Mol Biol 2011;709:75–89.

45. Clark KR, Liu X, McGrath JP, et al. Highly purified recombinant adeno-associated virus vectors are biologically active and free of detectable helper and wild-type viruses. Hum Gene Ther 1999;10: 1031–1039.

46. Pozsgai ER, Griffin DA, Heller KN, et al. Beta-sarcoglycan gene transfer decreases fibrosis and restores force in LGMD2E mice. Gene Ther 2016; 23:57–66.

47. Glen BB, Luke MJ, James MA, et al. The polyproline site in hinge 2 influences the functional capacity of truncated dystrophins. PLoS Genet 2010;6:e1000958.

48. Ramos JN, Hollinger K, Bengtsson NE, et al. - Development of novel micro-dystrophins with enhanced functionality. Mol Ther 2019;27:623–635.

49. Adams ME, Odom GL, Kim MJ, et al. Syntrophin binds directly to multiple spectrin-like repeats in

dystrophin and mediates binding of nNOS to repeats 16–17. Hum Mol Genet 2018;27:2978–2985.

50. Lai Y, Zhao J, Yue Y, et al. α2 and α3 helices of dystrophin R16 and R17 frame a microdomain in the α1 helix of dystrophin R17 for neuronal NOS binding. Proc Natl Acad Sci U S A 2012;110:525–530.
51. Chicoine LG, Montgomery CL, Bremer WG, et al. Plasmapheresis eliminates the negative impact of AAV antibodies on microdystrophin gene expression following vascular delivery. Mol Ther 2014; 22:338–347.
52. Chicoine LG, Rodino-Klapac LR, Shao G, et al. Vascular delivery of rAAVrh74.MCK.GALGT2 to the gastrocnemius muscle of the rhesus macaque stimulates the expression of dystrophin and laminin α2 surrogates. Mol Ther 2014;22:713–724.
53. Xu R, Jia Y, Zygmunt DA, et al. An isolated limb infusion method allows for broad distribution of rAAVrh74.MCK.GALGT2 to leg skeletal muscles in the rhesus macaque. Mol Ther Methods Clin Dev 2018;10:89–104.
54. Mendell JR, Sahenk Z, Lehman K, et al. Assessment of systemic delivery of rAAVrh74.MHCK7 .micro-dystrophin in children with Duchenne muscular dystrophy: A nonrandomized trial. JAMA Neurol 2020;77:1122–1131.
55. Zygmunt DA, Crowe KE, Flanigan KM, et al. Comparison of serum rAAV serotype-specific antibodies in patients with Duchenne muscular dystrophy, Becker muscular dystrophy, inclusion body myositis, or GNE myopathy. Hum Gene Ther 2017;28:737–746.
56. Duan D. Systemic AAV micro-dystrophin gene therapy for Duchenne muscular dystrophy. Mol Ther 2018;26:2337–2356.
57. Yoshimura M, Sakamoto M, Ikemoto M, et al. AAV vector-mediated microdystrophin expression in a relatively small percentage of *mdx* myofibers improved the *mdx* phenotype. Mol Ther 2004;10: 821–828.
58. Banks GB, Judge LM, Allen JM, et al. The polyproline site in hinge 2 influences the functional capacity of truncated dystrophins. PLoS Genet 2010;6:e1000958.
59. Mendell JR, Campbell K, Rodino-Klapac L, et al. Dystrophin immunity in Duchenne's muscular dystrophy. N Engl J Med 2010;363:1429–1437.
60. Talsness DM, Belanto JJ, Ervasti JM. Disease-proportional proteasomal degradation of missense dystrophins. Proc Natl Acad Sci U S A 2015;112: 12414–12419.
61. McCourt JL, Rhett KK, Jaeger MA, et al. In vitro stability of therapeutically relevant, internally truncated dystrophins. Skelet Muscle 2015;28:13.
62. Gao QQ, McNally EM. The dystrophin complex: structure, function, and implications for therapy. Compr Physiol 2015;5:1223–1239.
63. Lai Y, Thomas GD, Yue Y, et al. Dystrophins carrying spectrin-like repeats 16 and 17 anchor nNOS to the sarcolemma and enhance exercise performance in a mouse model of muscular dystrophy. J Clin Invest 2009;119:624–635.
64. Hakim CH, Wasala NB, Pan X, et al. A five-repeat micro-dystrophin gene ameliorated dystrophic phenotype in the severe DBA/2J-*mdx* model of Duchenne muscular dystrophy. Mol Ther Methods Clin Dev 2017;6:216–230.
65. Yue Y, Pan X, Hakim CH, et al. Safe and bodywide muscle transduction in young adult Duchenne muscular dystrophy dogs with adeno-associated virus. Hum Mol Genet 2015;24:5880–5890.
66. Percival JM, Anderson KN, Huang P, et al. Golgi and sarcolemmal neuronal NOS differentially regulate contraction-induced fatigue and vasoconstriction in exercising mouse skeletal muscle. J Clin Invest 2010;120:816–826.
67. Rebolledo DL, Kim MJ, Whitehead NP, et al. Sarcolemmal targeting of nNOSμ improves contractile function of *mdx* muscle. Hum Mol Genet 2016;25:158–166.
68. Crosbie RH, Straub V, Yun HY, et al. *mdx* muscle pathology is independent of nNOS perturbation. Hum Mol Genet 1998;7:823–829.
69. Chao DS, Silvagno F, Bredt DS. Muscular dystrophy in *mdx* mice despite lack of neuronal nitric oxide synthase. J Neurochem 1998;71:784–789.

Received for publication September 17, 2020
accepted after revision November 24, 2020

Published online: January 4, 2021

IMMAGINI SUPPLEMENTARI

Figure S1. Effect of systemic treatment with rAAVrh74.MHCK7.micro-dystrophin on transgene expression in all skeletal muscles. Representative immunofluorescent images of heart, diaphragm, psoas major (Psoas), tibialis anterior, gastrocnemius, quadriceps, triceps, and gluteus stained for micro-dystrophin using an N-terminal dystrophin antibody in wild-type mice, rAAVrh74.MHCK7.micro-dystrophin-treated *mdx* mice at the intermediate dose ($6x10^{12}$ vg total), and Lactated Ringer's (vehicle)-treated *mdx* mice (*mdx*-LR mice) 3 months post-injection.

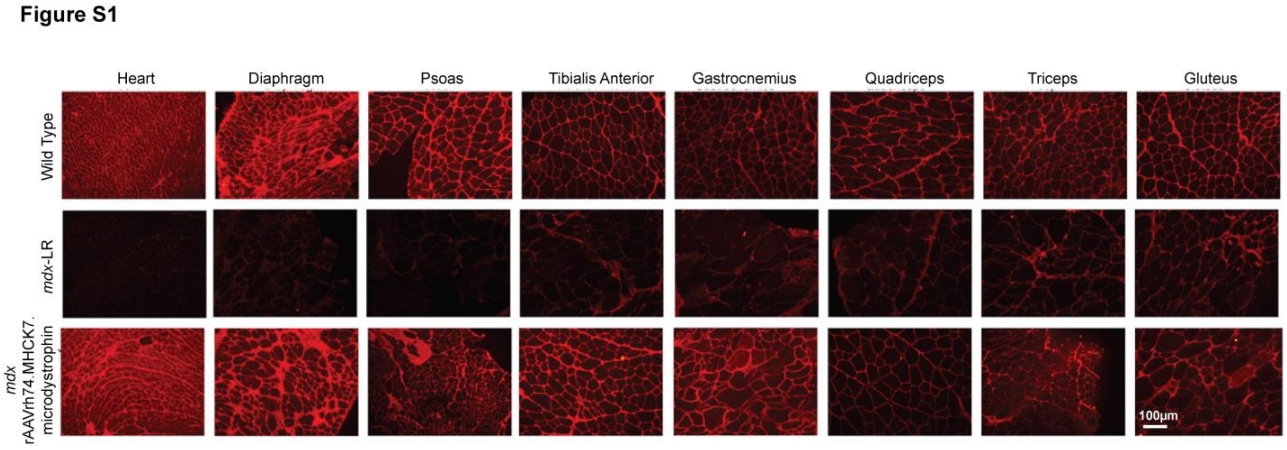

Figure S2. Effect of systemic treatment with rAAVrh74.MHCK7.micro-dystrophin on muscle pathology. (**A**) Hematoxylin and eosin stain of gastrocnemius, quadriceps, psoas major (Psoas), and gluteus muscle tissue from wild-type mice, Lactated Ringer's (vehicle)-treated *mdx* mice (*mdx*-LR mice), and rAAVrh74.MHCK7.micro-dystrophin-treated (intermediate dose, $6x10^{12}$ vg total) *mdx* mice. (**B**) Bar graphs represent quantification of fiber diameter represented in A; histograms represent the relative frequency distribution of the myofibers (n=4, low dose; n=8, intermediate and high dose; n=6, *mdx*-LR; and n=6, wild-type). Data are reported as mean +/- standard error of the mean. Data were analyzed by one-way ANOVA followed by Tukey's post hoc analysis. ****=p<0.0001 vs *mdx*-LR mice. ++= p<0.005; +++=p=0.001; ++++=p<0.0001 vs. wild-type (**C**) Quantification of percentage of muscle fibers with central nucleation (low dose, n=5; intermediate dose, n=6; and high dose, n=7; *mdx*-LR and wild-type, n=6). Data are reported as mean +/- standard error of the mean. Data were analyzed by two-way ANOVA followed by Tukey's post hoc analysis. ***=p<0.001, ****=p<0.0001 vs *mdx*-LR mice. Abbreviations: Dia, diaphragm; Gas, gastrocnemius; Glut, gluteus; Psoas, psoas major; Qd, quadriceps; TA, tibialis anterior; Tri, triceps.

Figure S2

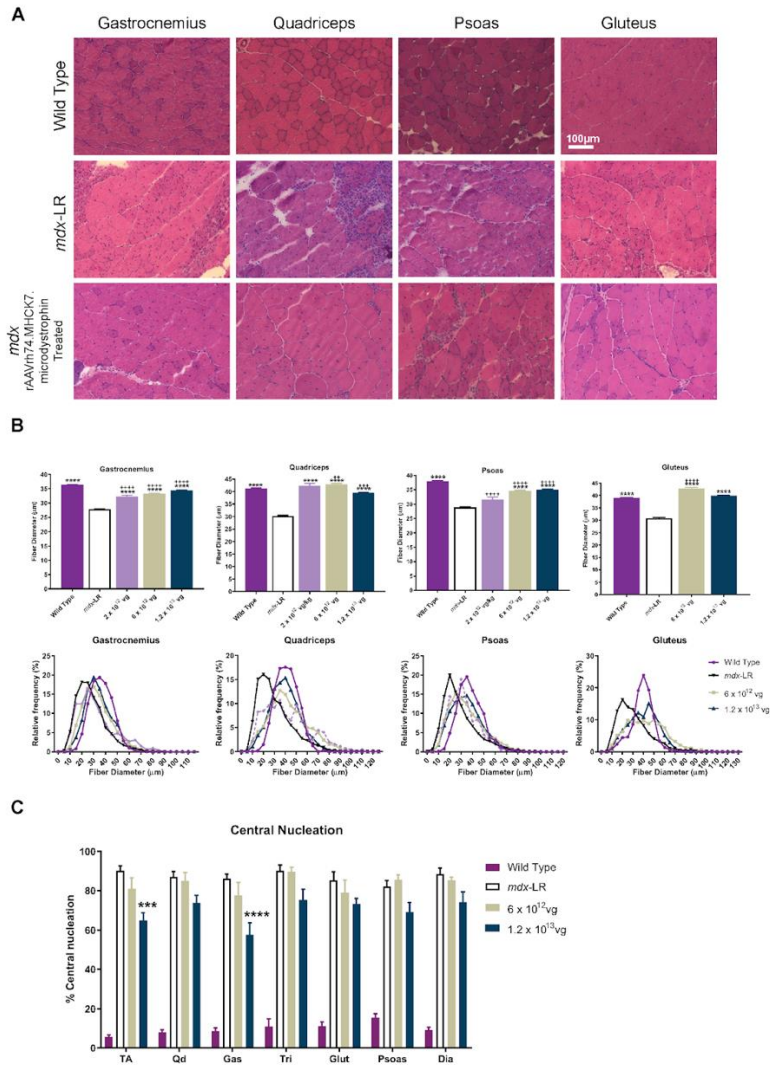

Figure S3. Absence of ringed fibers with the delivery of rAAVrh74.MHCK7.micro-dystrophin, which contains hinge 2 on ringed fibers. Representative images of gastrocnemius tissue stained with an alpha sarcomeric actin antibody to evaluate the presence or instance of ringed fibers in wild-type mice, Lactated Ringer's (vehicle)-treated *mdx* mice *(mdx*-LR mice), or rAAVrh74.MHCK7.micro-dystrophin-treated *mdx* mice (intermediate dose, $6x10^{12}$ vg total, construct contains Hinge 2). 20X images are shown.

Figure S3

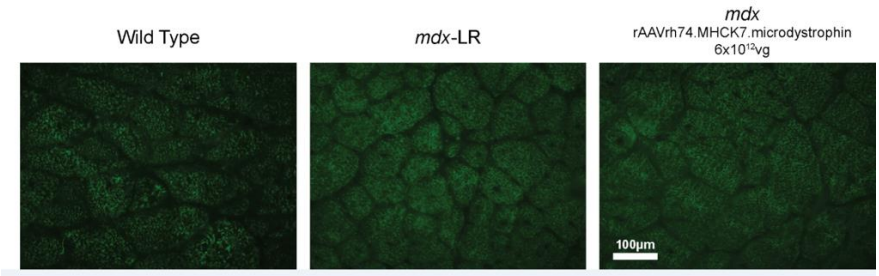

Figure S4. Lack of toxicity detected in a serum chemistry panel in mice after systemic treatment with rAAVrh74.MHCK7.micro-dystrophin. A serum chemistry panel was assessed from wild-type mice, Lactated Ringer's (vehicle)-treated *mdx* mice (*mdx*-LR mice), and *mdx* mice systemically treated with rAAVrh74.MHCK7.micro-dystrophin intermediate ($6x10^{12}$ vg), and high ($1.2x10^{13}$ vg) doses (n=5 to 8). Dotted lines represent upper and lower limits. Values beyond the limits are considered abnormal. Abbreviations: ALP/K, alkaline phosphatase; ALT, alanine aminotransferase; AST, aspartate aminotransferase; B/C, conjugated bilirubin; BUN, blood urea nitrogen; CREAT, creatinine; DBIL, direct bilirubin; GLU, glucose; TBIL, total bilirubin; TP, total protein.

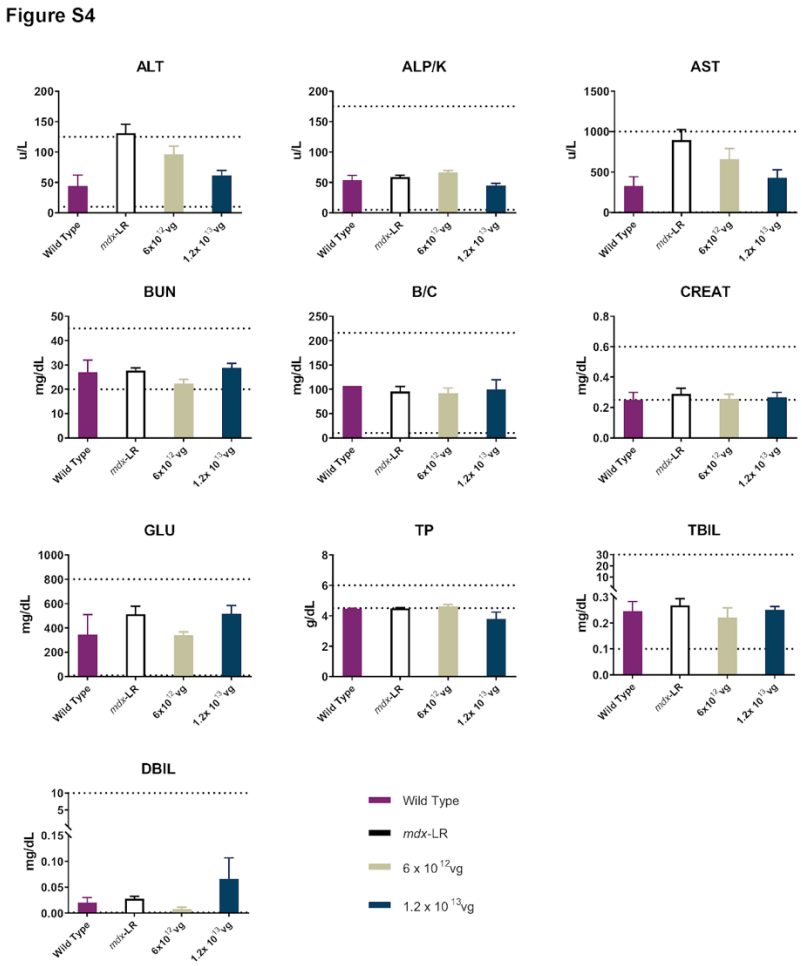

Figure S5. Full images of western blots shown in Figure 5B. (**A**) Western blot analysis of dystrophin protein expression in muscles from representative mouse 3 months after treatment with rAAVrh74.MHCK7.micro-dystrophin at an intermediate ($6x10^{12}$ vg, left) and high ($1.2x10^{13}$ vg, right) dose. (**B**) Western blot analysis of dystrophin protein expression in off-target organs from representative mouse 3 months after treatment with rAAVrh74.MHCK7.micro-dystrophin at intermediate ($6x10^{12}$ vg, left) and high ($1.2x10^{13}$ vg, right) dose. Abbreviations: Dia, diaphragm;

Gas, gastrocnemius; Glut, gluteus; Gon, gonads; Hrt, heart; Kid, kidney; Liv, liver; Lng, lung; Pso, psoas major; Qd, quadriceps; Spl, Spleen; TA, tibialis anterior; Tri, triceps; WT, wild-type.

Figure S5

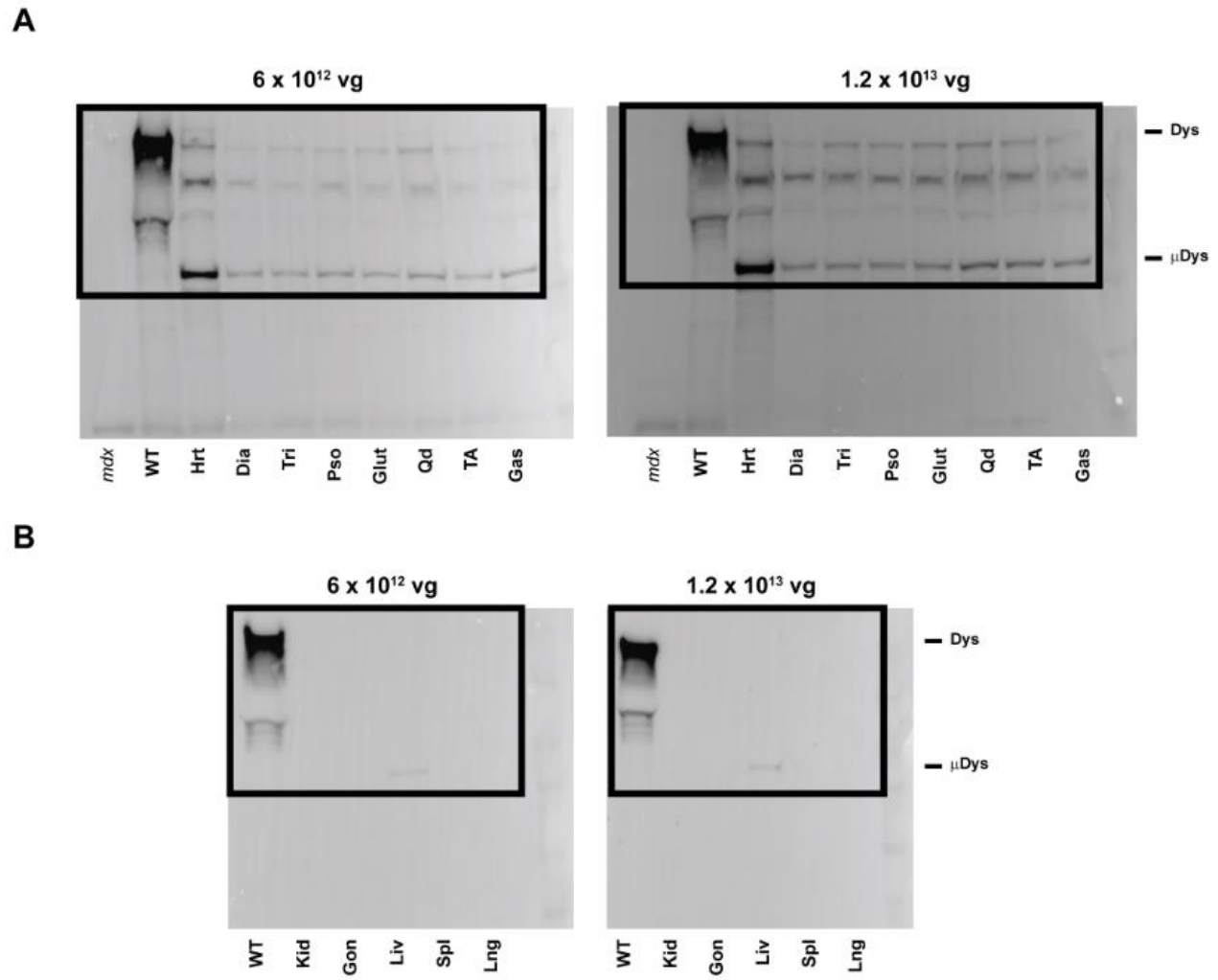

Figure S6. Full images of western blots from additional animals (Representative animal shown in Figure 5 and S5).

Western blot analysis of dystrophin protein expression in muscles 3 months after treatment with rAAVrh74.MHCK7.micro-dystrophin at an intermediate (Mouse 347 and Mouse 348 at $6x10^{12}$ vg, top) and high (Mouse 388 and Mouse 387 at $1.2x10^{13}$ vg, bottom) dose. Abbreviations: Dia, diaphragm; Gas, gastrocnemius; Glut, gluteus; Hrt, heart; Pso, psoas major; Qd, quadriceps; TA, tibialis anterior; Tri, triceps; WT, wild-type.

Figure S6

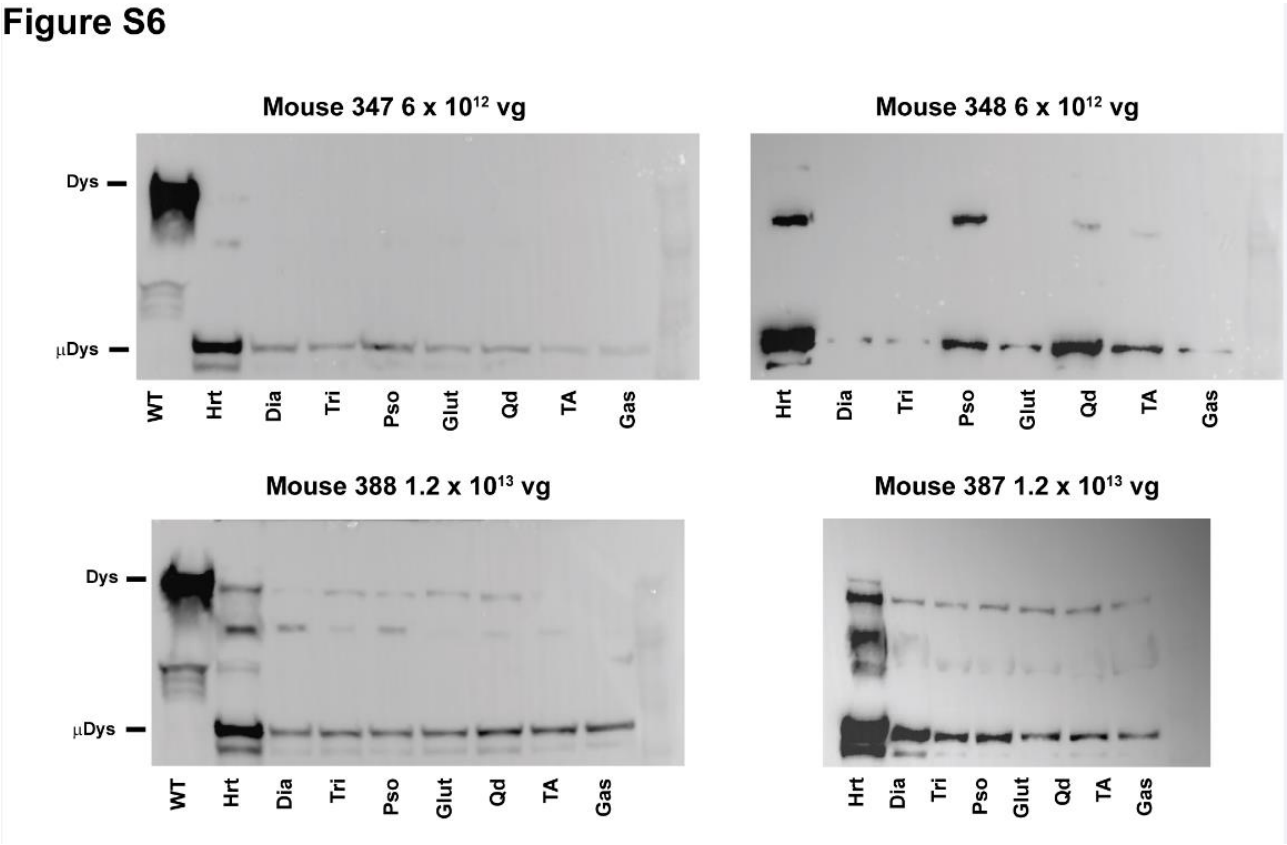

Table S1. Antibodies for immunohistochemistry and western blot

Primary antibody	Provider	Product number	Dilution WB	Dilution IF
Dystrophin primary antibody 4C7	Santa Cruz Biotechnology	sc-33697		1:50
Dystrophin primary antibody Dys1	Leica Biosystems	NCL-DYS1	1:50	
Dystrophin primary antibody Dys3	Leica Biosystems		1:20	
Human beta-sarcoglycan primary antibody	Leica Biosystems	B-SARC-L-CE		1:100
Neuronal nitric oxide synthase (nNOS) primary antibody	Fisher Scientific	61-7000	1:1,000	1:100
γ-tubulin antibody	Sigma	T6557	1:10,000	
α-actinin antibody	Sigma	F3777	1:10,000	1:10,000
Alexa Fluor 680 goat anti-mouse	Licor	926-68070	1:5,000	
Alexa Fluor 568 goat anti-mouse IgG2b	Invitrogen	A-11004		1:250